LLNL-TR-729408

Lawrence Livermore National Laboratory

DOSIMETRY CHARACTERIZATION OF THE GODIVA REACTOR UNDER BURST CONDITIONS

Hickman, D. P.[1], Heinrichs, D. P. [1], Hudson, R. [1], Wong, C. [1], Ward, D.[2], Wilson, C.[3], Clark, L. [3], Trompier, F.[4]

June 22, 2017

[1]Lawrence Livermore National Laboratory
[2]Sandia National Laboratories
[3]Atomic Weapons Establishment
[4]Institut de Radioprotection et de Sûreté Nucléaire

Disclaimer

INTRODUCTION

A series of sixteen (16) burst irradiations were performed in May 2014, fifteen of which were part of an international collaboration to characterize the Godiva IV fast burst reactor at the National Criticality Experiments Research Center (NCERC). Godiva IV is a bare cylindrical assembly of approximately 65 kg of highly enriched uranium fuel (93.2% ^{235}U metal alloyed with 1.5% molybdenum for strength) and is designed to perform controlled prompt critical excursions (Myers 2010, Goda 2013). Twelve of the irradiations were dedicated to neutron spectral measurements using a Bonner multiple sphere spectrometer. Three irradiations, with core temperature increases of 71.1°C, 136.9°C, and 229.9°C, were performed for generating comparative fluence data, establishing corrections for varying heights, testing linearity with burst temperature, and establishing gamma dose characteristics.

BURST INFORMATION

Most of the bursts were performed at a change in core temperature of approximately 70 °C. The average ΔT for these bursts was 69 ± 4 °C. Three bursts on 5/27 - 28/2014 were performed specifically for NAD and TLD exposures but also included isolated follow up multi-sphere spectrometer measurements. Table 1 provides the details of the bursts.

Table 1. Godiva characterization burst data (May 2014).

Burst Date	Burst Time	Burst ΔT (°C)	Increment (mils)	Period (μs)	Alpha (μs^{-1})	Reactivity (¢)
5/19/2014	14:29	65.9	56	62	0.016	101.9
5/20/2014	10:52	68.8	60	58.9	0.017	102.1
5/20/2014	14:38	65.1	59	67.3	0.015	101.8
5/21/2014	9:42	65.4	58	66.2	0.015	101.8
5/21/2014	13:00	70	63	56.3	0.018	102.1
5/21/2014	16:10	70.8	64	55.1	0.018	102.1
5/22/2014	9:55	69.9	63	53	0.019	102.2
5/22/2014	9:55	69.9	63	53	0.019	102.2
5/22/2014	13:01	70.6	64	55.1	0.018	102.1
5/22/2014	16:07	70.3	63	53	0.019	102.2
5/22/2014	16:07	70.3	63	53	0.019	102.2
5/27/2014	13:31	229.9	317	10.4	0.096	111.3
5/28/2014	10:53	136.9	199	17.2	0.058	106.9
5/28/2014	15:46	69.2	64	57.9	0.017	102
5/29/2014	10:15	71.1	65	NA	NA	NA
5/29/2014	13:45	68.5	64	58.9	0.017	102

CHARACTERIZATION METHODS

Two sets of measurement protocols were implemented to characterize the neutron field at Godiva. The first protocol consisted of a series of bursts that were performed at nearly the same temperature (delta T). A summary of the bursts used in this evaluation is provided in Appendix A. Nine Bonner Spheres of differing size were used to make a measurement at each of nine locations around Godiva. Each measurement was performed at approximately 70 degrees delta T with spheres being sequentially rotated among 9 characterization locations around Godiva. A description of the PBSS system, methods, and neutron spectral results are provided in (Wilson, et. al. 2014). Neutral fluence (n/cm^2) as derived from the neutron spectral results are provided in Appendix B.

The second protocol set was executed on 27-28 May 2014. The second protocol set consisted of the measurement of bursts using Nuclear Accident Dosimeters (NADs), Calcium Fluoride TLDs, Ion

Chambers, and Personnel Dosimeters at the nine characterization locations. The characterized locations are graphically represented in Fig. 1.

Fission foils were also deployed during both protocols as a part of the evaluation. The fission foils were positioned in the "Glory Hole" of Godiva adjacent to the core as a measure of the number of fissions.

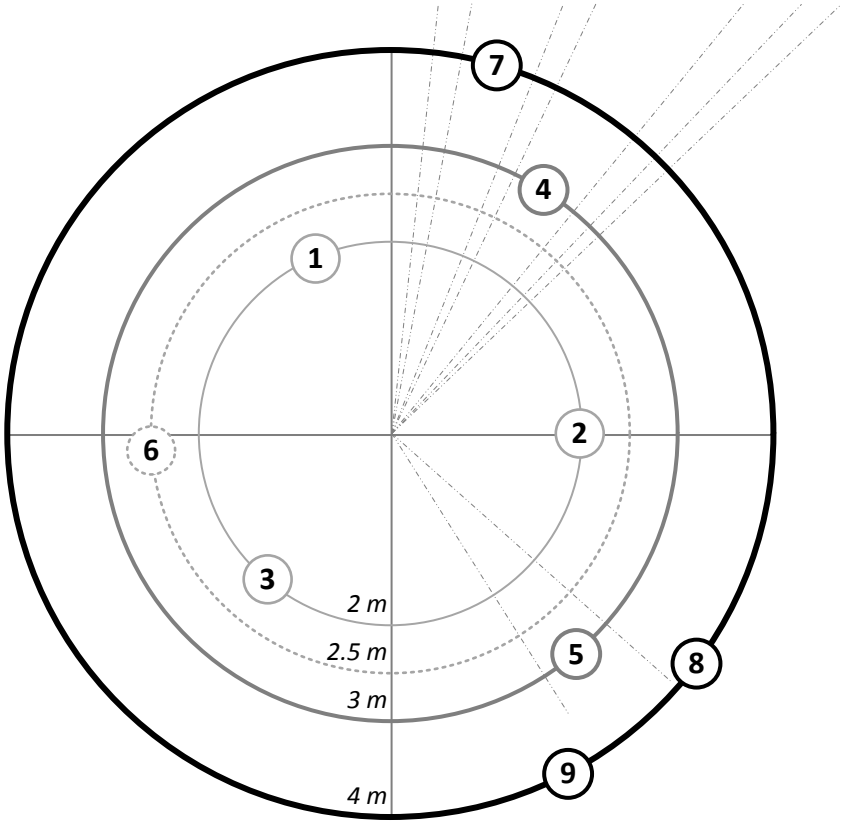

Figure 1. Characterized Neutron and Gamma Dose Positions around Godiva

Passive Neutron Bonner sphere Spectrometer Measurements

A Passive Bonner sphere Spectrometer (PBSS) was developed by AWE (Wilson, et. al. 2014) for the measurement of the Godiva-IV assembly in the pulsed mode. The detector element is a gold foil placed at the center of each polyethylene sphere; the foil is activated by the moderated neutron field and is measured later using a gamma-ray spectrometer. For a comprehensive description of the PBSS (multisphere) measurements refer to (Wilson, et. al. 2014).

The PBSS has nine spheres and for a complete measurement of the neutron spectrum at a reference location each sphere must be irradiated at that position. Since there were nine reference locations all of the spheres could be exposed simultaneously during each burst of the critical assembly and then moved

to another position for the next excursion. Due to the number of reactor operations required to collect a full data set the magnitude of the excursions was limited to that producing a core temperature of 70°C. The average temperature of the nine excursions was 68.5 +/- 2.4°C (@ 1σ) but all the measurement data was normalized to 70°C, equivalent to approximately 1×10^{16} fissions.

Neutron Nuclear Accident Dosimeter (NAD) Measurements

LLNL Personnel NADs

LLNL deployed four hundred thirty-two (432) Nuclear Accident Dosimeters (NAD) as part of the evaluation of the Godiva fields. Four dosimeters were position on each aluminum plate at measurement locations 1 – 9. The dosimeters were position at the top row of the holding plates. Four different heights were evaluated for uniformity of response. The height of the Godiva core is 180 cm; thus, the data to calculate the effective distance for each plate from the Godiva assembly as illustrated in Figure 2 and are provided in the Table 2.

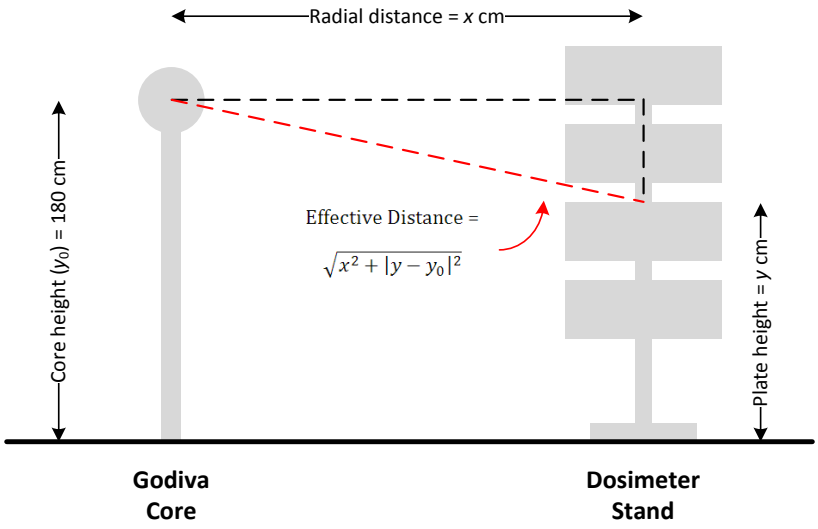

Figure 2. Calculation of Effective Distance between Reactor Core and Dosimeter (from Tai, 2016).

Table 2. Heights and Effective Distances of dosimeter holding plates.

Position	Position Distance from Core (m)	Plate ID	Top of Plate Height (cm)	Effective Distance from Core (cm)
1 - 3	2	AB	197	200.7
		CD	156	201.4
		EF	115	210.3
		GH	70.5	228.0
6	2.5	AB	220	253.2
		CD	169.5	250.2
		EF	119.5	257.2
		GH	69	273.5
4 & 5	3	AB	220	302.7
		CD	169.5	300.2
		EF	119.5	306.0
		GH	69	319.9
7 - 9	4	AB	234	403.6
		CD	178.5	400.0
		EF	123	404.0
		GH	67.5	415.5

Dosimeters were deployed for three burst levels: 229.9, 136.9, and 71.1 °C. Activities per unit mass were evaluated for each activation foil and sulfur pellet. From the decay corrected activity per unit mass measurements the fluence is determined. Calculated activity per unit mass for indium foils situated at 2 meters from the core is shown Figure 3. Indium in the LLNL NAD design measure fluence from neutrons >1 MeV. The activity of the activated foil decreases as the NAD is placed closer to the floor. Geometrical correction would indicate that because of the increased distance from the core the correction at 2 meters for the 115 cm and 70.5 cm should be approximately 91% and 78% of the activities obtained at upper plates (AB &CD) respectively.

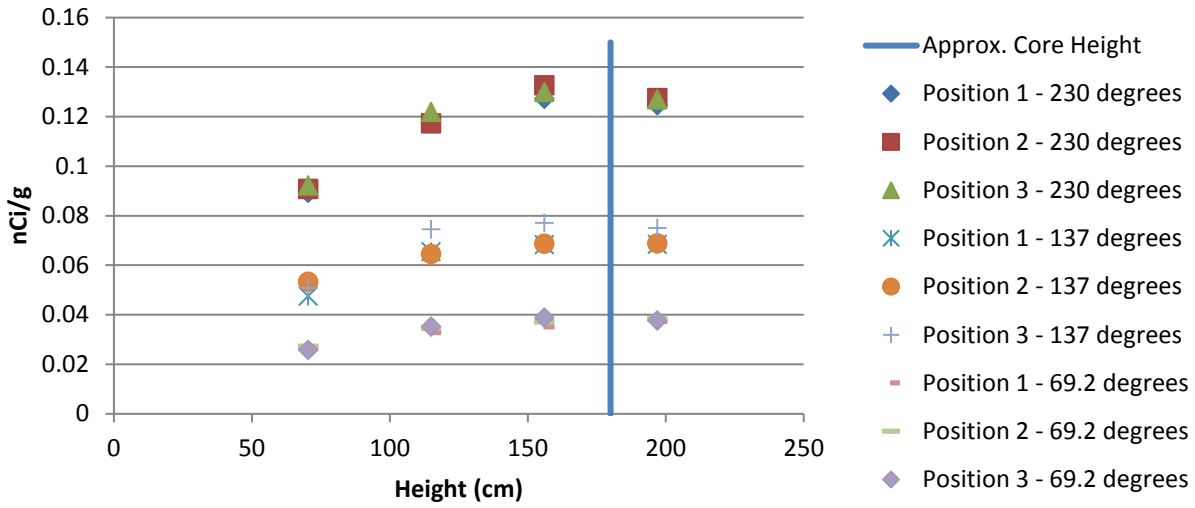

Figure 3. Average LLNL NAD ^{115m}In activity caused by (1 MeV neutrons and above) at various heights on an aluminum stand positioned 2 meters from the core.

The influence on the total fluence as a function of the effective distance is shown in Figure 4. However, as the position gets further from the core of the reactor there is an apparent increase in the amount of scatter as indicated by the lack of an expected inverse square relationship.

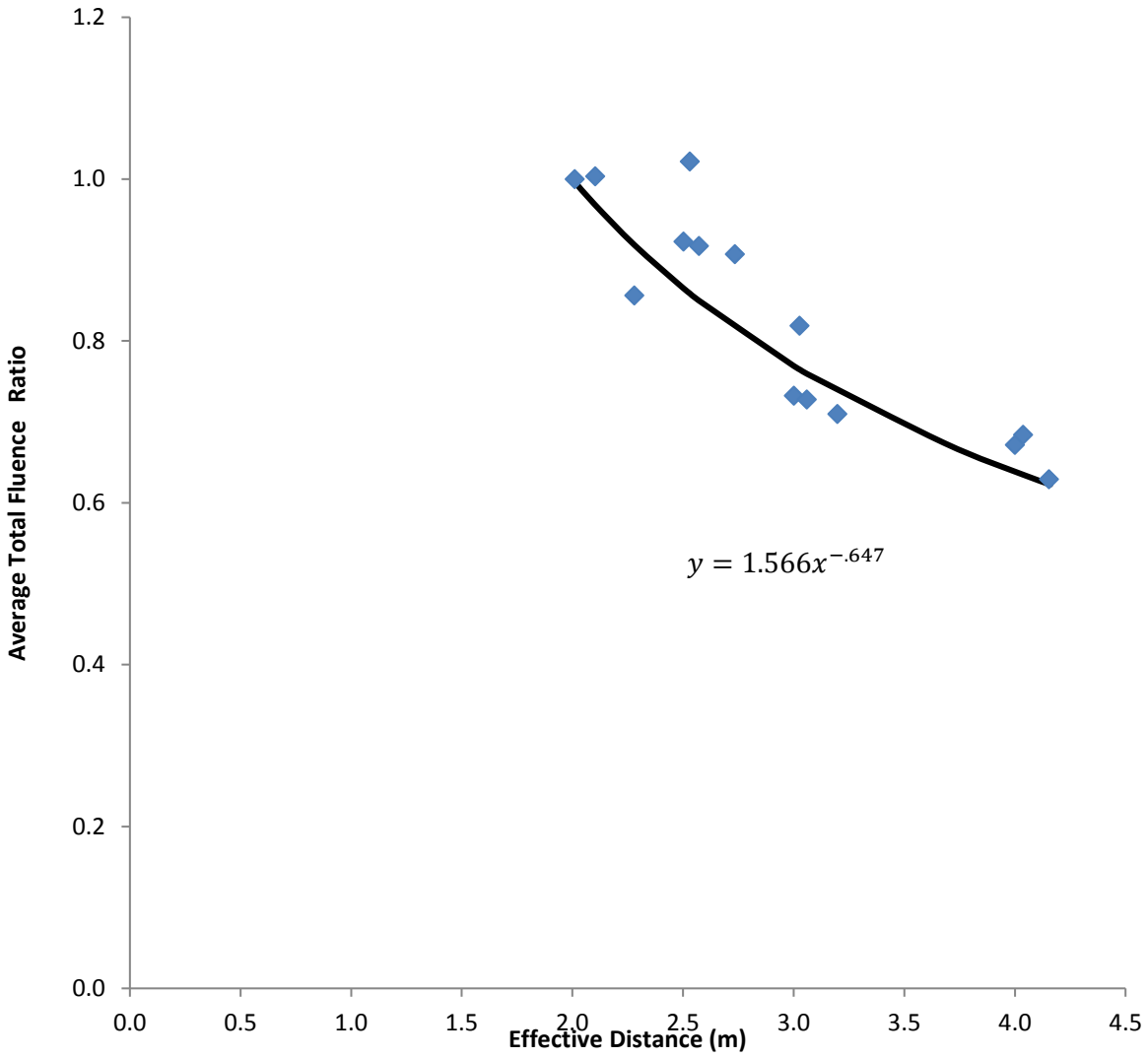

Figure 4. Ratio of average fluence to the average fluence at 2 meters from the reactor as a function of height (effective distance), including the effective distance for varying heights of dosimeters.

Figure 5 provides an example of the effects of the effective distance on fluence when dosimeters were placed on an aluminum stand positioned at 3 meters. As demonstrated in Figure YY, the observed effects of distance for a specific energy range can be significantly different from that observed for the total fluence.

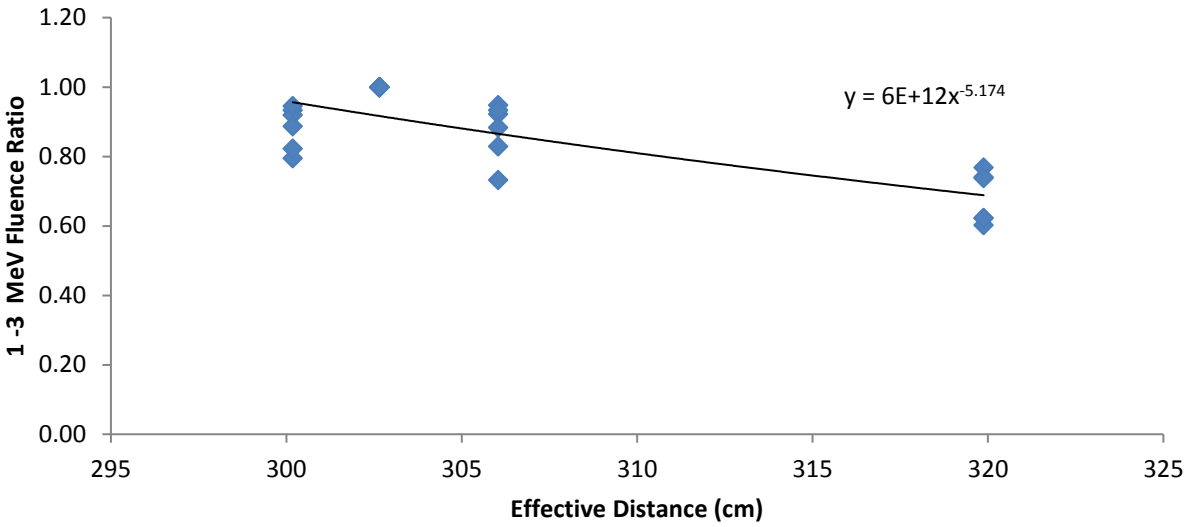

Figure 5. Ratio of average fluences (relative to highest most unobstructed position on stand) on 3 meters from the core of the reactor versus effective distance (height) for the 1 to 3 MeV energy range.

At stand positions greater than 3 meters from the core (i.e., 4 meters), the effect of height (effective distance) appears to have minimal or no effect as shown in Figure 6. This result indicates that no correction for the effective distance is required when the dosimeters are positioned at the 4-meter isopleth.

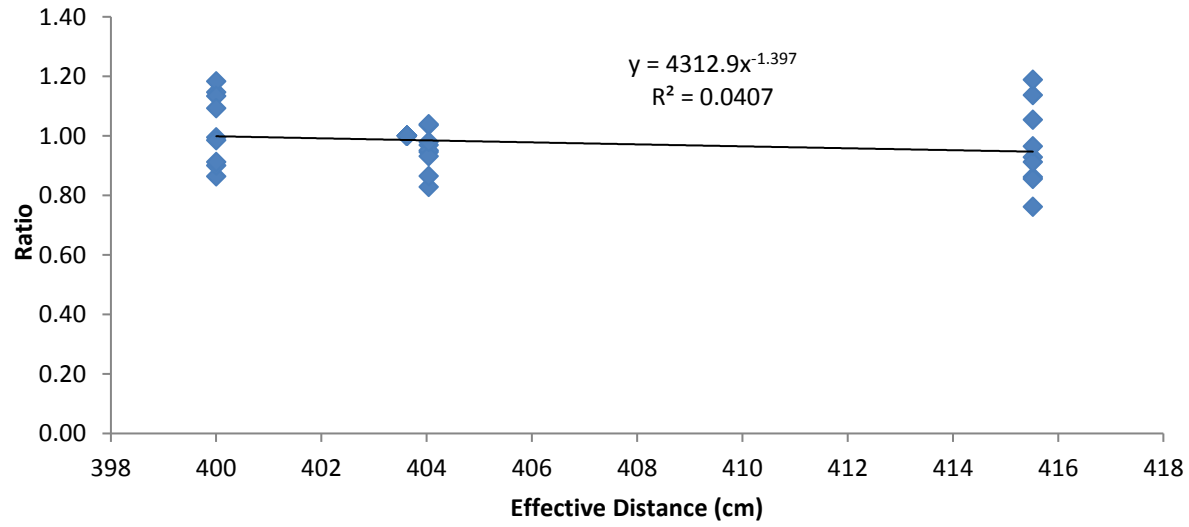

Figure 6. Ratio of average fluences (relative to highest most unobstructed position on stand) on 4 meters from the core of the reactor versus height on the stand (effective distance) for the 1 to 3 MeV energy range.

Figures 7a – d demonstrate the change in fluence as a function of height for each energy range monitored using the LLNL nuclear criticality accident dosimeter. These ranges are Thermal, 1eV to 1MeV, 1-3 MeV, and >3 MeV. As seen in the figures, only neutron energies beyond 1 MeV appear to vary with height (effective distance) on the stand up to 4 meters. For energies below 1 MeV, it appears that the scatter component of the spectrum is consistent, regardless of the height (effective distance).

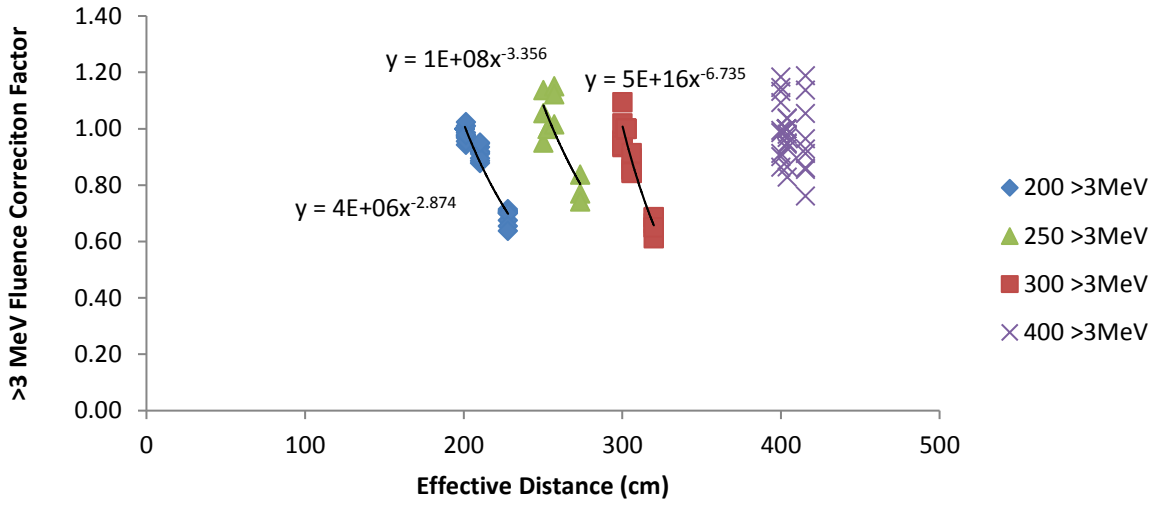

Figure 7a. Ratio of average fluence (relative to highest most unobstructed position on stand) versus height (effective distance) on stands at 2, 2.5, 3, and 4 meters for the > 3 MeV energy range.

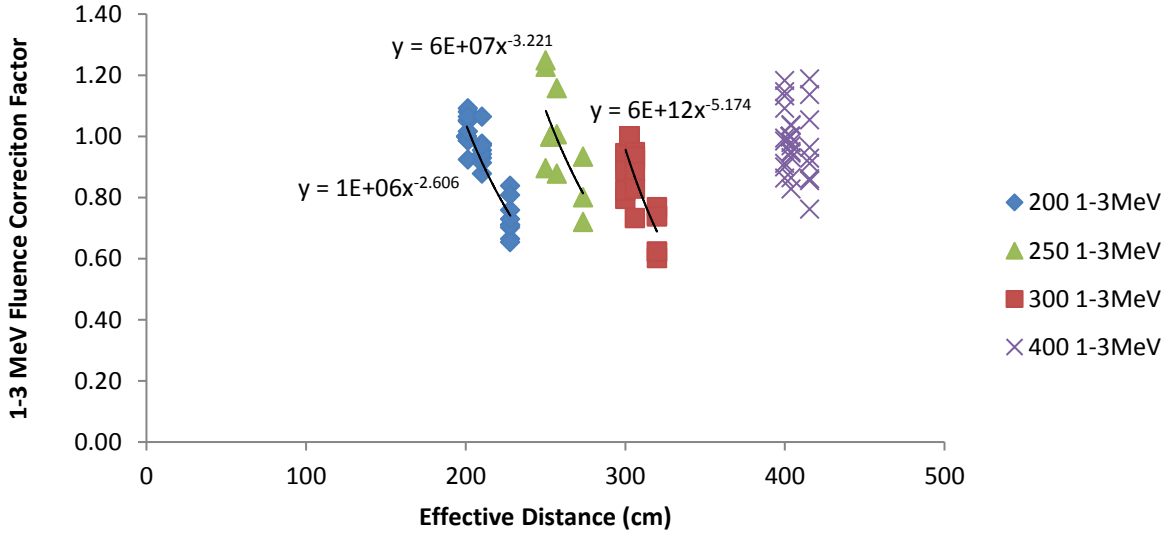

Figure 7b. Ratio of average fluence (relative to highest most unobstructed position on stand) versus height (effective distance) on stands at 2, 2.5, 3, and 4 meters for the 1 - 3 MeV energy range.

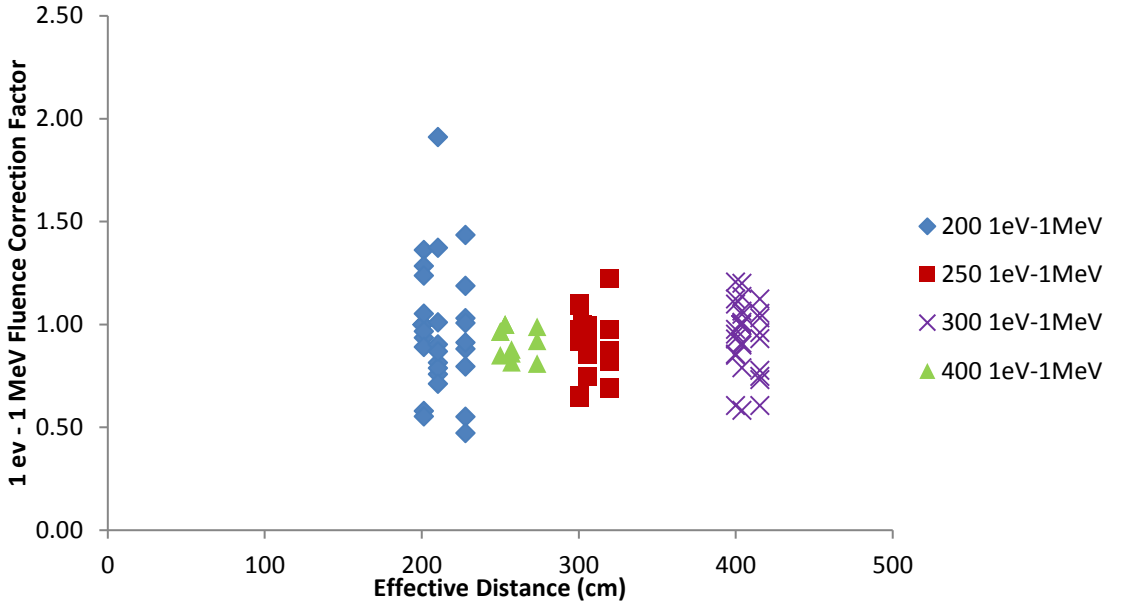

Figure 7c. Ratio of average fluence (relative to highest most unobstructed position on stand) versus height (effective distance) on stands at 2, 2.5, 3, and 4 meters for the 1 eV - 3 MeV energy range.

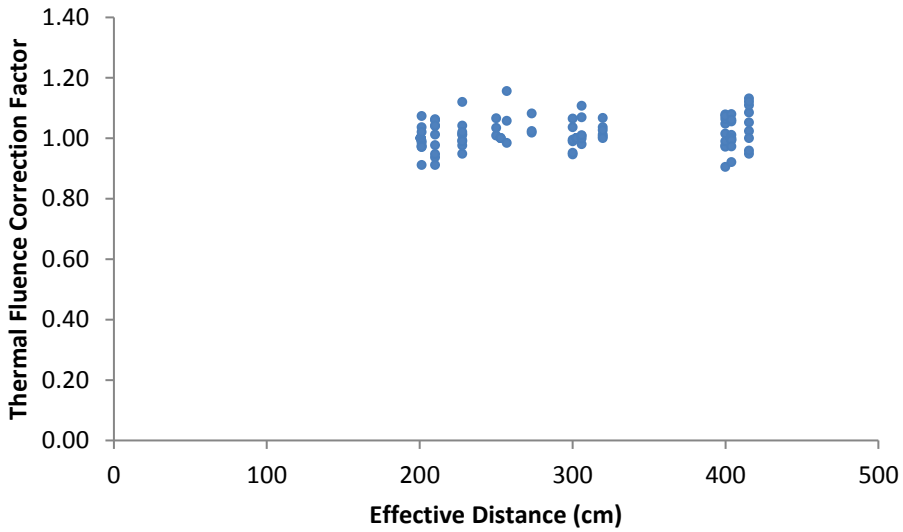

Figure 7d. Ratio of average fluence (relative to highest most unobstructed position on stand) versus height (effective distance) on stands at 2, 2.5, 3, and 4 meters for the thermal energy range.

Figures 7c and 7d show that the fluence (and dose) does not change with height (effective distance) for the 1 eV – 1 MeV and thermal energy ranges. In contrast, out to 4 meters, there are significant changes

in the fluence for >1 MeV neutrons with height. Using the correction factors in Figures 7a and 7b the change in the fluence and dose as a function of height is evaluated. Table 3 demonstrates that the fluence and neutron tissue kerma dose can change by as much as 9.4% and 20% respectively at a height of 69 cm.

Equations for establishing height correction factors:

Neutron Energy Range[1]	Center of Stand Distance (m)[2]	Correction Factor Equation[a]
1-3 MeV	2	$Y = 1\times10^{6}X^{-2.606}$
	2.5	$Y = 6\times10^{7}X^{-3.221}$
	3	$Y = 6\times10^{12}X^{-5.174}$
>3 MeV	2	$Y = 4\times10^{6}X^{-2.874}$
	2.5	$Y = 1\times10^{8}X^{-3.356}$
	3	$Y = 5\times10^{16}X^{-6.735}$

[a] Where *X* is the effective distance in cm as evaluated using Figure 2.

Table 3. The change in total fluence and neutron tissue kerma dose evaluated at the reactor core height (180 cm) and at a distance 69 cm from the floor for a 68.5 °C burst.

	Fluence (n/cm^2)		kerma (Gy)	
Stand Distance (m)	@180cm height	@69cm height	@180cm height	@69cm height
2	9.71E+10	8.80E+10	1.55E+00	1.24E+00
2.5	8.41E+10	7.87E+10	1.15E+00	9.65E-01
3	6.53E+10	6.02E+10	9.0E-01	7.21E-01
4	5.19E+10	5.30E+10	6.5E-01	6.50E-01

Using spectral data established from PBSS measurements performed by Wilson, et.al., the average fluence (and error) at the 2, 2.5, 3, and 4 meter distances 180 cm from the floor for a 68.5 °C burst are provided in Table 4.

[1] No correction is indicated for neutron energies below 1 MeV.
[2] No correction is indicated at 4 meters.

Table 4. Average fluence (1.6E-9 to 14 MeV) and neutron tissue kerma for a 68.5°C burst, 180 cm from floor.

Distance	Average fluence (n/cm^2)	+/-	1s	Average kerma (Gy)[3]	+/-	1s
2m	9.71E+10	+/-	2.78%	1.55	+/-	2.23%
2.5m	8.41E+10	+/-	NA	1.15	+/-	NA
3m	6.53E+10	+/-	2.40%	0.90	+/-	2.40%
4m	5.19E+10	+/-	3.49%	0.65	+/-	3.24%

Fixed NADs

Fixed nuclear activity dosimeters contain the same materials and shielding design as the personnel nuclear accident dosimeters. However, the fixed NADs have larger foils and provide more sensitivity and better counting statistics than the personnel NADs. Because the fixed NADs contain more material there are higher activity levels after irradiation and they can be measured at times further out from the event. The Fixed NADs were measured after the Personnel NADs (PNADs) were completely measured, thus reducing the degree of accuracy. Corrections for height (as described above) were applied to Fixed NADs to correct results for the exact stand distance (2, 2.5, 3, and 4 meters). The expected results are based on spectrum measurements. The average difference from the expected for the FNADs is provided in Table 5.

Table 5. Average difference (observed versus expected fluence) for the LLNL FNADs.

Distance	Avg. Difference
2	-12.79%
2.5	0.59%
3	-21.56%
4	-2.52%

AWE Personnel NADs

Fluence data from the AWE NADs was evaluated and derived using the same energy bins as the LLNL NADs, >3 MeV, 1 – 3 MeV, 1 eV – 1 MeV, and Thermal energies. Specific data about the AWE NADs can be obtained from Wilson et. al. The AWE NADs were exposed to a 229.9°C burst of the Godiva reactor. Comparison of fluence results for the AWE and LLNL NADs indicate that there is a 6.8% difference between the averaged results of the two styles of NADs as seen in Figure 8.

[3] Average kerma values from Wilson, et. al. is 1.51, 1.12, 0.88, 0.63 Gy for the 2m, 2.5m, 3m, and 4m distances respectively.

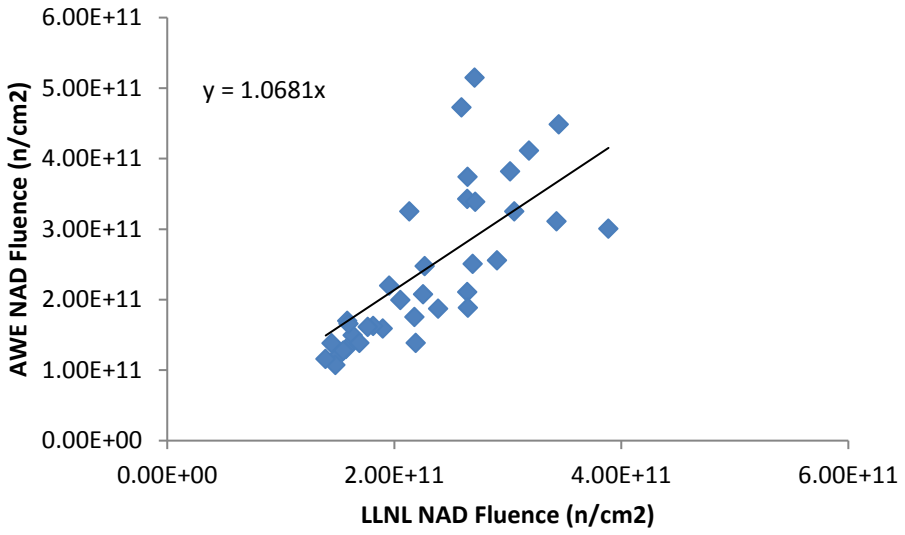

Figure 8. Comparison of fluence results for AWE and LLNL NADs exposure to a 229.9°C burst of the Godiva reactor.

A paired t-test two tailed P-value equals 0.3648 with 35 degrees of freedom. By conventional criteria, the difference between the two data sets is considered not statistically significant.

SNL Personnel NADs

Indium foils in the SNL Personnel NADs evaluated the dose for neutron energies above 1 MeV. Foils were irradiated at 2, 3, and 4 meters. Average Element 57 doses (Gy) for foils irradiated at least 180 cm above the floor are presented. Expected Element 57 doses are based on the AWE spectral measurements for neutron energies above 1MeV and dose factors from Auxier, et.al. SNL neutron dose results are presented in Table 6.

Table 6. Element 57 dose comparison for SNL Personnel NADs (>1 MeV).

Distance (m)	Average Element 57 Dose (Gy)	Error (±1s)	Expected	% Difference
2	3.64	0.14	3.73	-2%
3	2.15	0.11	2.03	6%
4	1.31	0.31	1.42	-8%

IRSN NADs

Eleven Nuclear Accident Dosimeters from the Institute of Nuclear and Radiation Safety (IRSN) were irradiated to the 229.9 °C burst. The positions of the dosimeters are provided in Table II. The day after the irradiation, the dosimeters were sent to the France/IRSN via overnight mail. Because of uncontrollable delays in delivery to IRSN, only neutron tissue kerma and photon doses could be

provided since the gold foils used for thermal neutron evaluation had decayed too much. Background doses were estimated and subtracted from the results since the control dosimeters were also irradiated. The neutron tissue kerma and photon absorbed doses are provided in Tables 8 and 11 respectively.

Table 7. IRSN NAD locations for the 229.9 °C Burst of Godiva.

Dosimeter ID	Floor Position	Distance (m)	Plate-Location	Bottom of Plate Height from Floor (cm)
AMB 000	1	2	B-7	166.5
AMB 001	2	2	B-7	166.5
AMB 002	3	2	B-7	166.5
AMB 003	4	3	B-7	189.5
AMB 004	5	3	B-7	189.5
AMB 005	6	2.5	B-7	189.5
AMB 006	7	4	B-7	203.5
AMB 007	8	4	B-7	203.5
AMB 008	9	4	B-7	203.5
AMB 009	6	2.5	D-7	189.5
TEMOIN 000	2	2	A-8	166.5

Each IRSN NAD was comprised of a RPL Glass dosimeter (used for the photon dose component) and an alanine dosimeter used to measure the neutron tissue kerma.

Comparison of Average PBSS (Multisphere) Spectrometer, LLNL, AWE, and IRSN NAD data

LLNL PNADs and AWE Lockets were positioned on aluminum stands at 2, 2.5, 3. And 4 meters for the 230 °C ΔT burst. Comparison of fluence between LLNL and AWE NADs located on the top plates (Plates A&B) is provided in Table CC2 for the 229.9-degree burst.

Table 8. Average neutron tissue kerma doses using the Multi-sphere neutron spectrometer, LLNL NAD, AWE Locket, and IRSN NAD.

	Average neutron tissue kerma (Gy)			
Distance (m)	PBSS	LLNL NAD	AWE Locket	IRSN NAD
2	4.94	5.04	5.12	5.7
2.5	3.67	4.02	3.39	3.9
3	2.87	3.00	2.73	3.4
4	2.29	2.09	1.67	2.4

On average, the data from the AWE Locket, IRSN NAD, and LLNL PNADs were within ±10% of the PBSS (multisphere) Spectrometer tending to confirm the known values for the neutron tissue kerma.

Table 9 presents comparisons to the Element 57 and the ANSI 13.3 doses using the measured neutron spectrum for Godiva and the NADs used by AWE and LLNL. These data demonstrate dose consistency to within 15% and typically within a few percent.

Table 9. Element 57 and ANSI 13.3 neutron dose comparisons for a 229.9 °C burst of Godiva.

	Element 57 Average Dose[4] (Gy)			ANSI 13.3 Average Dose (Gy)			
Distance (m)	PBSS	AWE Locket	LLNL NAD	Reference D (10)	LLNL NAD D (10)	Reference D*(10)	LLNL NAD D*(10)
2	6.18	6.07	6.26	6.64	6.42	6.41	6.18
2.5	4.71	4.21	4.96	5.03	5.17	4.84	4.93
3	3.69	3.60	3.60	3.93	3.73	3.78	3.59
4	2.71	2.29	2.62	2.88	2.72	2.76	2.60

Neutron Dose Relationship to the Number of Fissions

Fission foil measurements were performed for each of the irradiations as well as in April of 2014. Additional fission foil measurements were performed in May 2016 resulting in the availability of 26 measurements of the total number of fissions. The neutron tissue kerma dose was evaluated using PBSS (multisphere) estimated doses at a height of the core relative to the Burst ΔT for each2 6 measured fission foils. The resulting measured average neutron tissue kerma relative to the number of fissions is presented in Table 10. Calculated neutron tissue kerma was performed by the AWE[5]. The Caliban data was reported in Radiation Measurements 43 (2008) pages 1077 – 1080.

Table 10. Neutron tissue kerma as a function the number of fissions at the height of the Godiva reactor core.

	Measured kerma (Gy per 1E16 fissions)	Calculated kerma (Gy per 1E16 fissions)	
Distance (m)	Godiva-IV	Godiva-IV	Caliban
2	1.00	1.06	1.09
2.5	0.74	0.79	NA
3	0.58	0.62	0.59
4	0.42	0.44	0.41

[4] Element 57 doses based on IAEA 211 dose conversion values.
[5] Private communication with Chris Wilson, AWE.

Gamma Dose Measurements

Calcium Fluoride TLD Measurements

Sandia National Laboratory placed 10 CaF_2 Thermal Luminescent Dosimeters (TLDs) on each aluminum plate of the stands (a.k.a. trees) holding NADs, Pencil Ion Chambers, etc. Stands with CaF_2 TLDs were placed at all nine locations for three burst irradiations at 229.9 °C, 136.9 °C, and 71.1 °C. Plate heights and stand positioning are provided in Table 2 above. Figure Z shows a typical 2 meters set of results for a two-meter position.

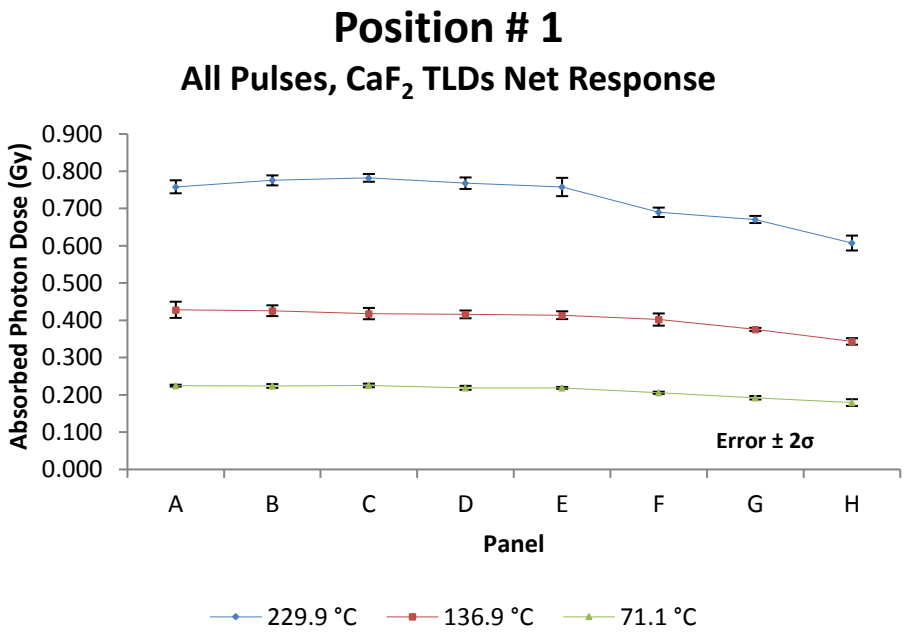

Figure 9. Absorbed photon dose (in Gy) for Position 1 (@ 2m) as a function of mounting Panel ID (height) using CaF_2.

A slight change in the photon dose occurs when dosimeters are positioned on lower plates. Using the effective distance method previously described and used for neutron corrections a correction to the photon dose as a function of effective distance and burst temperature can be made using the equation provided in Figure 10.

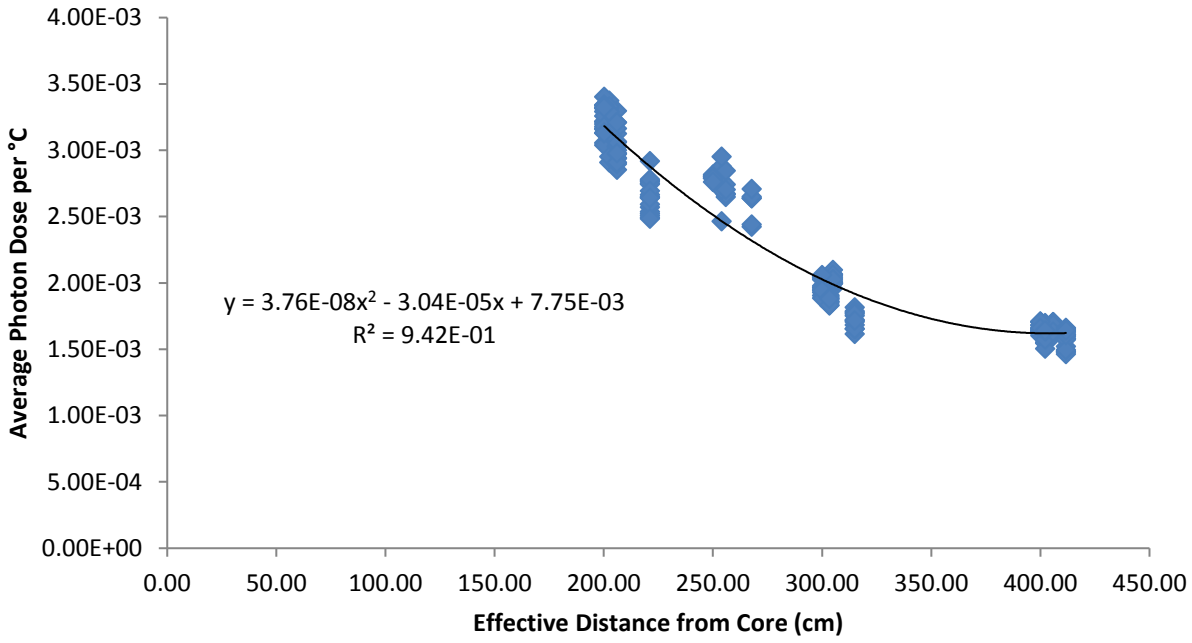

Figure 10. Correction function for photon dose per °C of burst temperature as a function of the effective distance.

Using the correction method established with the SNL CaF_2, the dose from the AWE and Personnel Ion Chamber dosimeters are compared for a 229.9 °C burst.

Table 11. Comparison of measured and predicted photon tissue doses for the 229.9 °C burst.

Location	Distance (m)	Average AWE TLD Photon Dose (Gy)	Average IRSN Photon Absorbed Dose (Gy)	SNL RADCAL Gamma Dose (Gy)	Predicted Photon Dose from CaF_2 (Gy)	PICs[6]
1 - 3	2	0.63	0.63	0.66	0.73	0.73
6	2.5	0.51	0.62		0.57	0.57
4,5	3	0.44	0.44		0.46	
7 - 9	4	0.33	0.36		0.37	0.34

Personnel Ionization Chamber Measurements

[6] Personnel Ionization Chambers

For the 229.9 degree burst the PICs provided excellent estimation of the photon dose as provided in Table 11 and shown in Figure 11. On average, the PICs provided doses that were within 5% of the CaF_2 results. Dosimetry results from the IRSN dosimeters, AWE dosimeters, and the Radcal ion chamber provided doses within 14% of the CaF dosimeters.

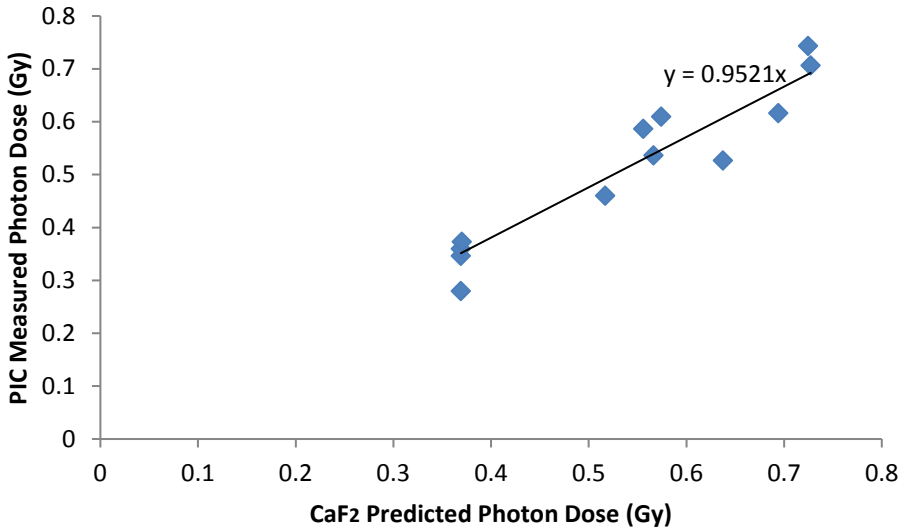

Figure 10. Personnel Ion Chamber (PIC) Photon dose relative the predicted photon dose based on CaF_2 measurements.

RADCAL Ion Chamber Measurements & Delayed Gamma Evaluation

A 0.6cc ion chamber connected to an integrating RADCAL digital monitor was placed in between the top of the A-B plated at Position 1, 2 meters away from the Godiva core for each of the three bursts (229.9, 136.9, and 71.1 °C). Personnel Ion Chambers (a.k.a. Pencil Chambers) were also placed near to the 0.6 cc ion chamber. The RADCAL readings for the 229.9 °C burst appear to be consistent with the CaF_2 readings, however the readings from the other two bursts are not consistent with the CaF_2 readings. Past studies with Godiva have demonstrated a strong EMF signal when the system is pulsed. It is possible that there were EMF influences on the Radcal monitor.

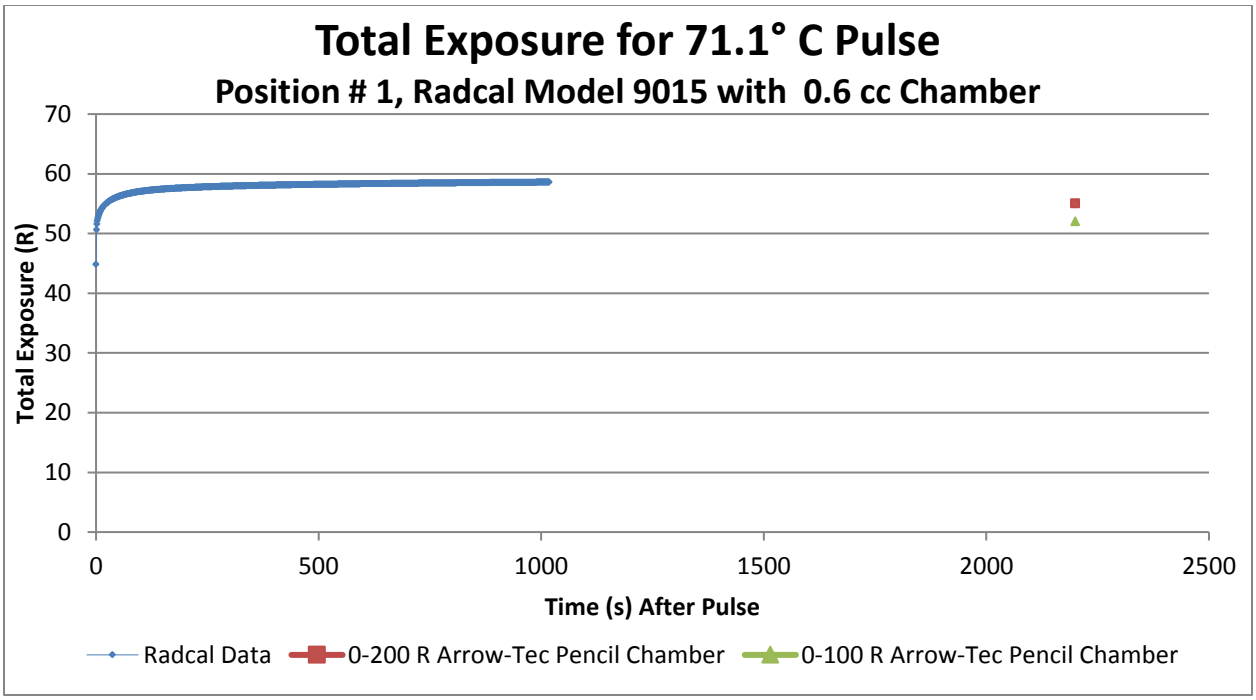
Total Exposure for 71.1° C Pulse
Position # 1, Radcal Model 9015 with 0.6 cc Chamber
Total Exposure (R)
0
10
20
30
40
50
60
70
0
500
1000
1500
2000
2500
Time (s) After Pulse
Radcal Data
0-200 R Arrow-Tec Pencil Chamber
0-100 R Arrow-Tec Pencil Chamber

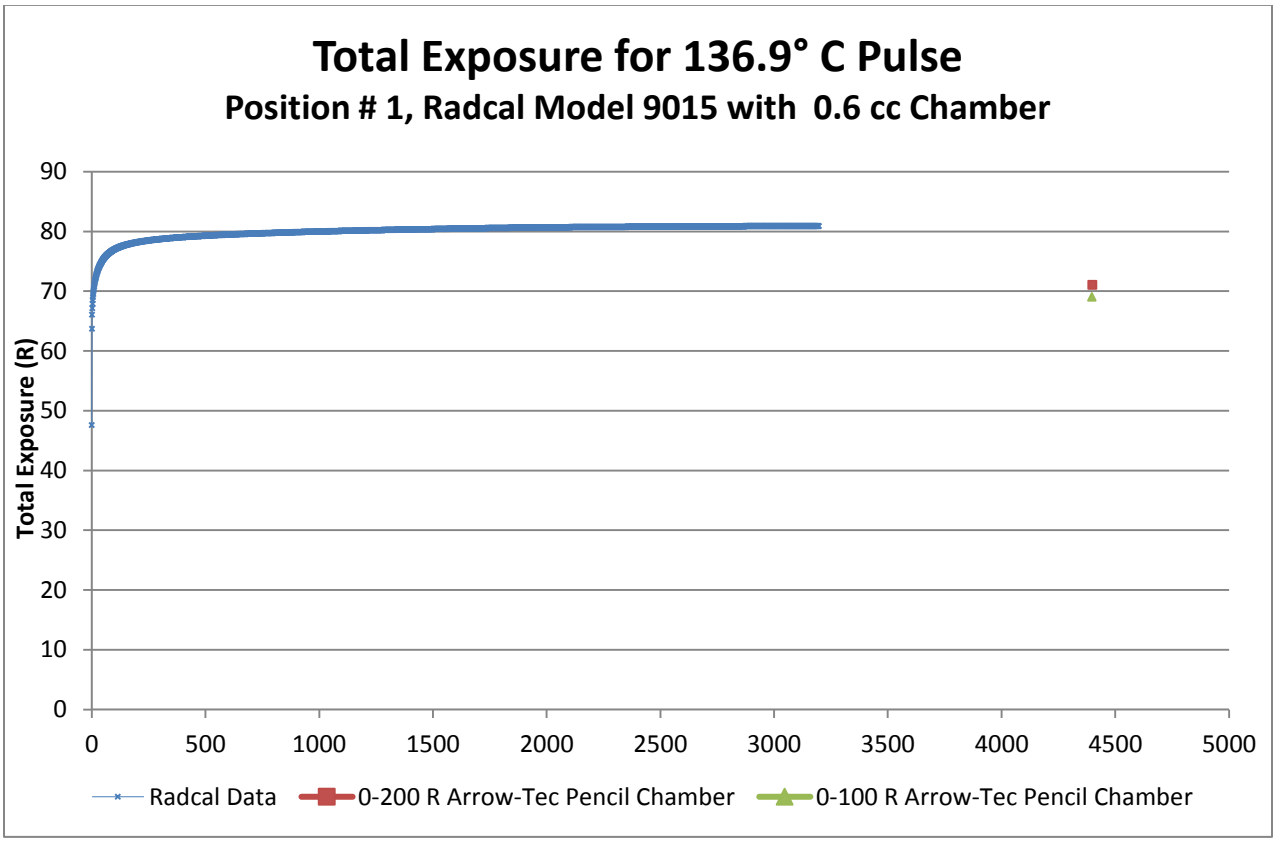
Total Exposure for 136.9° C Pulse
Position # 1, Radcal Model 9015 with 0.6 cc Chamber
Total Exposure (R)
0
10
20
30
40
50
60
70
80
90
0
500
1000
1500
2000
2500
3000
3500
4000
4500
5000
Radcal Data
0-200 R Arrow-Tec Pencil Chamber
0-100 R Arrow-Tec Pencil Chamber

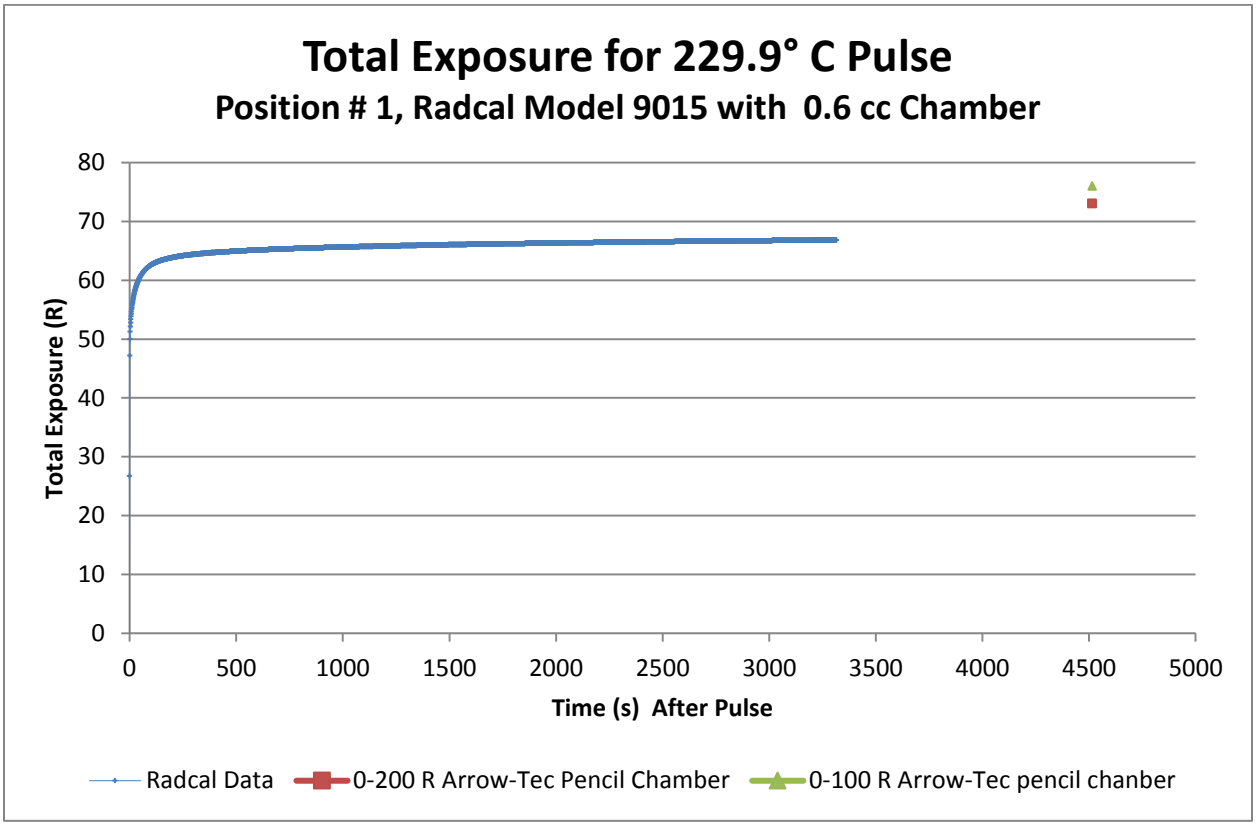

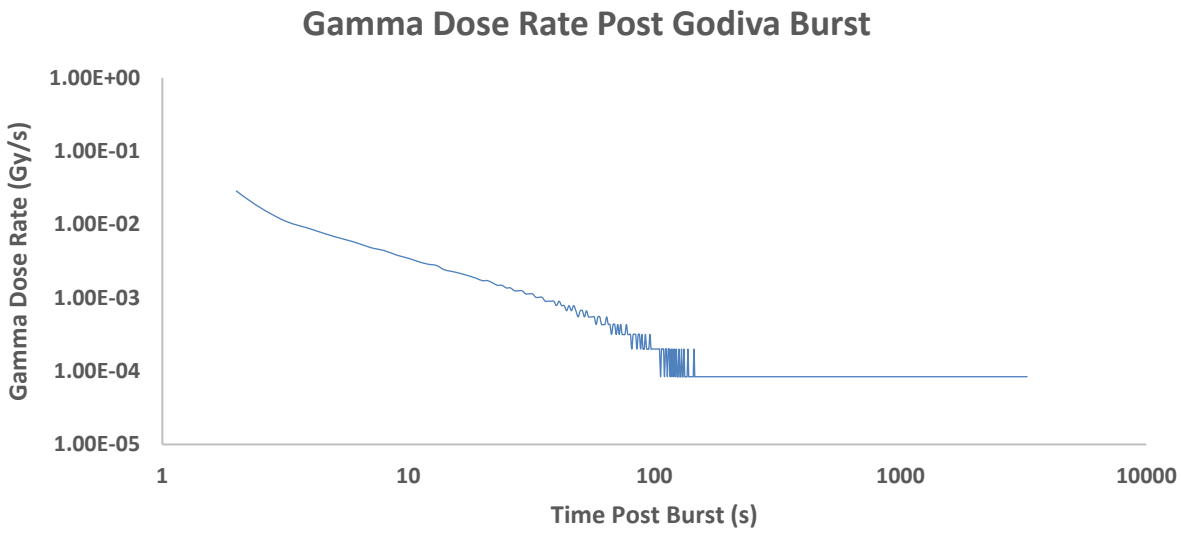

Differential measurement of the second by second gamma dose rate (See graph of Gamma Dose Rate Post Godiva Burst) after the burst show that 97.1 percent of the post burst gamma dose is accumulated within the first 120 seconds. Over the remaining 3157 seconds before retrieval of the dosimeters only

2.99% of the post burst gamma dose came from delayed gammas. There is more than a two-order reduction in the dose rate over the first 120 second post burst. This rapid decline in the dose rate demonstrates that the delayed gamma component is considered to have an insignificant effect on the estimation of total gamma dose. Retrieval of any dosimetry materials most likely will happen significantly the 120 seconds, but since the delayed gamma component has an insignificant effect on the total (prompt plus delayed) gamma dose, no corrections need to be made. Even if there was a doubling of the time for dosimeter retrieval (e.g., 2 hours), the delayed gamma component would be minimal compared to the dose from the prompt gamma burst and first 120 seconds of delayed gamma exposure.

Discussion of Reference Values

Neutron spectral data (neutron lethargy) was used to establish the fluence over the energy range of 1.58 E-9 to 8.04 MeV using multiple Bonner style spheres (Wilson, et.al. 2014). Nine bursts with core temperature increases of approximately 70 °C were used to characterize nine locations at 180 cm height around the Godiva core. Three locations were at 2 meters, one location was at 2.5 meters, two locations at 3 meters, and three locations at 4 meters. The Bonner sphere measurements demonstrated that fluence measurements at the same distance (e.g., 2 meters) were typically within 5% to 6% of each other. PNAD and AWE Locket measurements support the Bonner sphere fluence measurements and had similar results for fluence and dose.

Multiple LLNL PNADs were placed at various heights along the concentric measurement distances 2, 2.5, 3, and 4 meters. The LLNL PANDs confirmed that the corrections for height are necessary for neutron energies greater than 1 MeV at closer in distances. Sets of correction equations were derived from the PNAD data to better characterize the fluence at heights other than 180 cm.

Measurements of the photon doses performed by SNL using CaF_2 TLD chips were used to derive a function for predicting the photon dose as a function of the burst temperature and effective distance from the core. Personnel Ion Chambers that were placed near to the CaF_2 TLDs confirmed the CaF_2 doses and AWE photon dose estimates tended to support the CaF_2 doses.

References

Auxier, J.A., Snyder, W.S., Jones, T.D., *Neutron Interactions and Penetration in Tissue*, in Radiation Dosimetry Vol 1 *Fundamentals*, F. Attix and W.C. Roesch editors, Academic Press, 1968.

ANSI/HPS N13.3-2013, *Dosimetry for Criticality Accidents*, American National Standards Institute Inc./Health Physics Society, December 2013.

IAEA, *Dosimetry for Criticality Accidents*, IAEA Technical Report Series No. 211, International Atomic Energy Agency, Vienna, 1982.

Tai, Lydia, *Use of CR-39 for Nuclear Criticality Accident Dosimetry and High Neutron Dose Monitoring*, Master's Thesis, Oregon State University, October 26, 2016.

Trompier, F., Huet, C., Medioni, R., Robbies, I., Asselineau, B., *Dosimetry of mixed field irradiation facility CALABAN*, Radiation Measurements, Vol 43, pp 1077 – 1080, 2008.

Wilson, C., Clark, L., Angus, P., *Neutron spectrometry results from phase two of the Godiva-IV characterization*, AWE Report No. 880/14, November 2014.

Appendices

Appendix A. Godiva Burst Data – LLNL Studies

Burst Date[7]	Burst Time	Burst ΔT (°C)	Increment (mils)	Period (μs)	Alpha (μs^{-1})	Reactivity (¢)
4/15/2014	10:47	75.4	57	59.4	0.01683502	102
4/15/2014	16:02	129.2	164	19.2	0.05208333	106
4/16/2014	14:00	236.9	300	10.8	0.09259259	111
5/19/2014	14:29	65.9	56	62	0.01612903	101.9
5/20/2014	10:52	68.8	60	58.9	0.01697793	102.1
5/20/2014	14:38	65.1	59	67.3	0.01485884	101.8
5/21/2014	9:42	65.4	58	66.2	0.01510574	101.8
5/21/2014	13:00	70	63	56.3	0.01776199	102.1
5/21/2014	16:10	70.8	64	55.1	0.01814882	102.1
5/22/2014	9:55	69.9	63	53	0.01886792	102.2
5/22/2014	9:55	69.9	63	53	0.01886792	102.2
5/22/2014	13:01	70.6	64	55.1	0.01814882	102.1
5/22/2014	16:07	70.3	63	53	0.01886792	102.2
5/22/2014	16:07	70.3	63	53	0.01886792	102.2
5/27/2014	13:31	229.9	317	10.4	0.09615385	111.3
5/28/2014	10:53	136.9	199	17.2	0.05813953	106.9
5/28/2014	15:46	69.2	64	57.9	0.01727116	102
5/29/2014	10:15	71.1	65			
5/29/2014	13:45	68.5	64	58.9	0.01697793	102

[7] Bursts from 19-May-2014 through 29-May-2015 were used for the evaluation of spectra, fluence, and doses from Godiva.

Appendix B. Total Fluence and Dose (normalized to 70°C ΔT) at 180 cm above the floor.

	POSITION								
	1	2	3	4	5	6[8]	7	8	9
Total Fluence (n/cm2)	1.03E+11	9.80E+10	1.03E+11	6.69E+10	6.92E+10	8.77E+10	5.21E+10	5.45E+10	5.58E+10
Tiss. kerma Dose (Gy)	1.63E+00	1.57E+00	1.62E+00	1.19E+00	9.2E-01	9.4E-01	6.6E-01	6.8E-01	6.8E-01
ANSI 13.3 Dp(10) - Gy	2.18E+00	2.09E+00	2.18E+00	1.63E+00	1.26E+00	1.29E+00	9.1E-01	9.4E-01	9.4E-01
ANSI 13.3 D*(10) - Gy	2.11E+00	2.02E+00	2.10E+00	1.57E+00	1.21E+00	1.24E+00	8.8E-01	9.1E-01	9.2E-01
Auxier et. al. Element 57 (Gy)	2.09E+00	2.00E+00	2.08E+00	1.56E+00	1.21E+00	1.24E+00	8.8E-01	9.1E-01	8.7E-01
IAEA 211 (Gy)	2.02E+00	1.94E+00	2.01E+00	1.51E+00	1.17E+00	1.19E+00	8.5E-01	8.7E-01	8.8E-01
NCRP 38 (Gy)	2.13E+00	2.04E+00	2.12E+00	1.60E+00	1.24E+00	1.26E+00	9.0E-01	9.3E-01	9.4E-01

Appendix C. Nuclear Accident Dosimeter (NAD) Measurements

A large number of NADs were deployed by various laboratories. LLNL provided the greatest coverage of the field and their data will be used to assess the variation in the field, and the associated dose as a function both of the vertical displacement from the floor of the cell and the horizontal displacement from the reference location. LLNL also deployed NADs for three excursions with different magnitudes of fissions and is therefore able to assess the linearity of the dose as a function of the core temperature or number of fissions. AWE provided NADs for a single pulse and these will be compared to the LLNL data to assess the accuracy and precision of the measurement method, since the AWE NAD is a different

[8] Position 6 is at 2.5 meters from the core. Positions 3 & 4 are at 3 meters from the core.

design but one that utilizes similar materials and properties. NSTEC and SNL also provided NADs for exposure.

LLNL Personnel NADs

The current LLNL Personnel Nuclear Accident Dosimeter (PNAD) design was developed in 1984 **Invalid source specified.**.This design assures that the PNAD is compatible with the Panasonic TLD badge combination. The components of the PNAD badge combination are similar to the PNAD materials previously used at LLNL. Bare and cadmium shielded gold foils are used to measure the fluence of thermal neutrons (0.025 eV). Copper foils shielded by boron-loaded plastic are used for the measurement of intermediate energy neutrons (1eV to 1 MeV). Indium foils shielded by boron-loaded plastic neutrons with energies greater than 1 MeV, respectively; a sulfur pellet is used to measure neutron energies greater than 3 MeV. Performance of the new PNAD complies with system performance requirements in ANSI N13.3 'American National Standard for Criticality Accidents' **Invalid source specified.**. Finally, the design includes an unshielded indium foil for rapidly obtaining approximate dose estimates (Quick Sorting) to distinguish exposed persons from unexposed persons at or above 10 rad of dose.

The LNL design provides a four-channel spectrometer of the neutron field, allowing for changes in dose estimates as the neutron field changes. Figure A3-1 shows the basic design of the LLNL dosimeter.

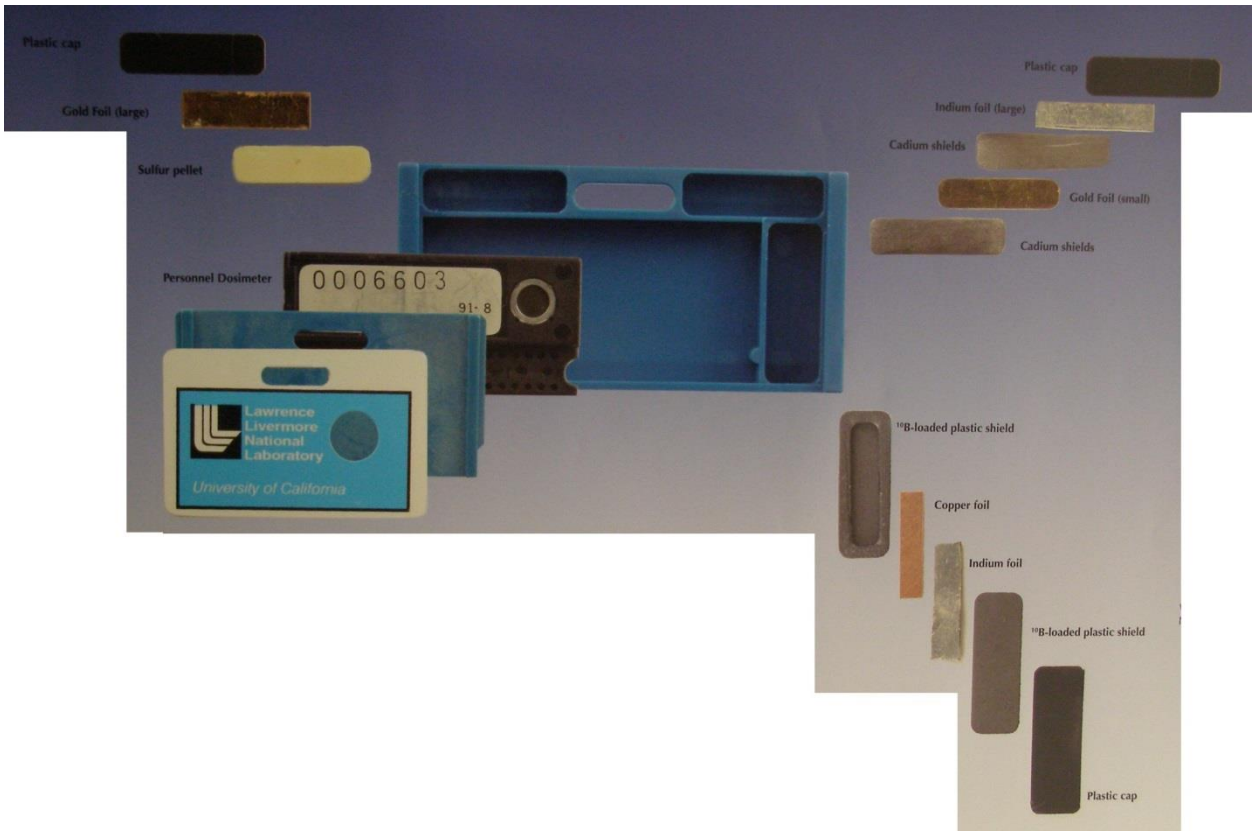

Figure C1. LLNL Nuclear Accident Dosimeter configuration.

AWE Personnel NADs

The NAD used at AWE comprises a plastic "locket" containing a sulphur tablet, an indium foil and two thin gold foils separated by a cadmium disc (see Figure for an illustration). AWE deployed 48 NADs for a single excursion of Godiva with a recorded core temperature of 230°C; this was the largest pulse undertaken during the characterization campaign. The NADs were located close to the centre of each aluminum plate; for the reference locations at 2 m two NADs were placed side-by-side on each plate; for more distant reference locations only a single locket was placed on each plate. After the irradiation the sulphur element of the NADs was counted using a gross beta counter and the other elements were assayed using a high-purity germanium gamma-ray spectrometer.

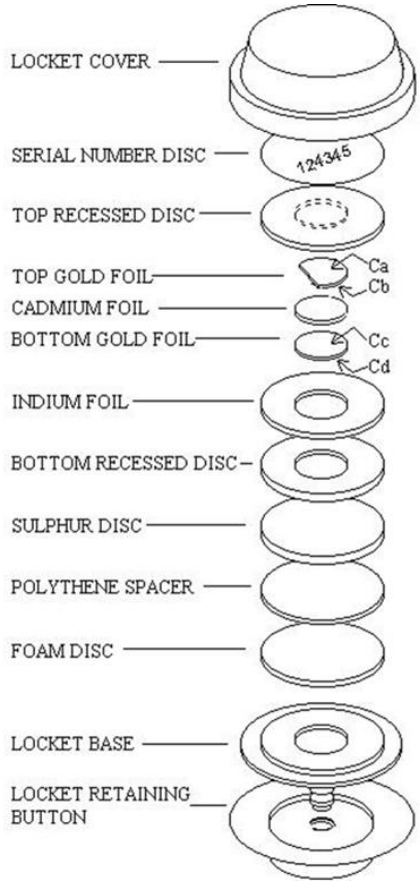

Figure C2: A schematic of the AWE personnel NAD showing the individual detector elements and their housing.

The neutron-induced activities measured in the locket elements were combined using an unfolding method developed by AWE and response functions generated using an MCNP6 model of the NAD (Wilson, et.al. 2014). The parameterized spectrum for each NAD was folded with fluence-to-dose conversion coefficients for neutron tissue kerma, Element 57 heavy-recoil dose and Element 57 total surface absorbed dose (IAEA, 1982).

Comparison of AWE and LLNL NADs

The AWE and LLNL NADs have several detector materials in common. The sulphur and indium elements are comparable, though they have different geometries that require alternate neutron fluence calibration factors. The gold elements have different shielding in each of the NADs and therefore cannot be compared easily. The interpretation of the neutron-induced activity in the Sulphur and Indium differs between the laboratories but the measured specific activity should be similar.

Neutron-induced P-32 activity

The Sulphur component in the AWE NAD is a disc with diameter 2.2 cm and thickness 0.24 cm; the same component in the LLNL NAD is a pellet 20.7 mm long, 5.6 mm wide and 4.0 mm thick. The ^{32}P specific activities measured in the sulphur components of both LLNL and AWE for all locations and heights are shown in Figure . There is a clear linear relationship between the two measurands but the specific activity in the AWE sulphur component is 1.3 times greater than the equivalent activity in the LLNL component. Two possible explanations for this are; a difference in the calibration factor relating the measured beta activity to total activity; or, a difference in the neutron-induced activity resulting from the difference in the cross-sectional area of the component facing the neutron field.

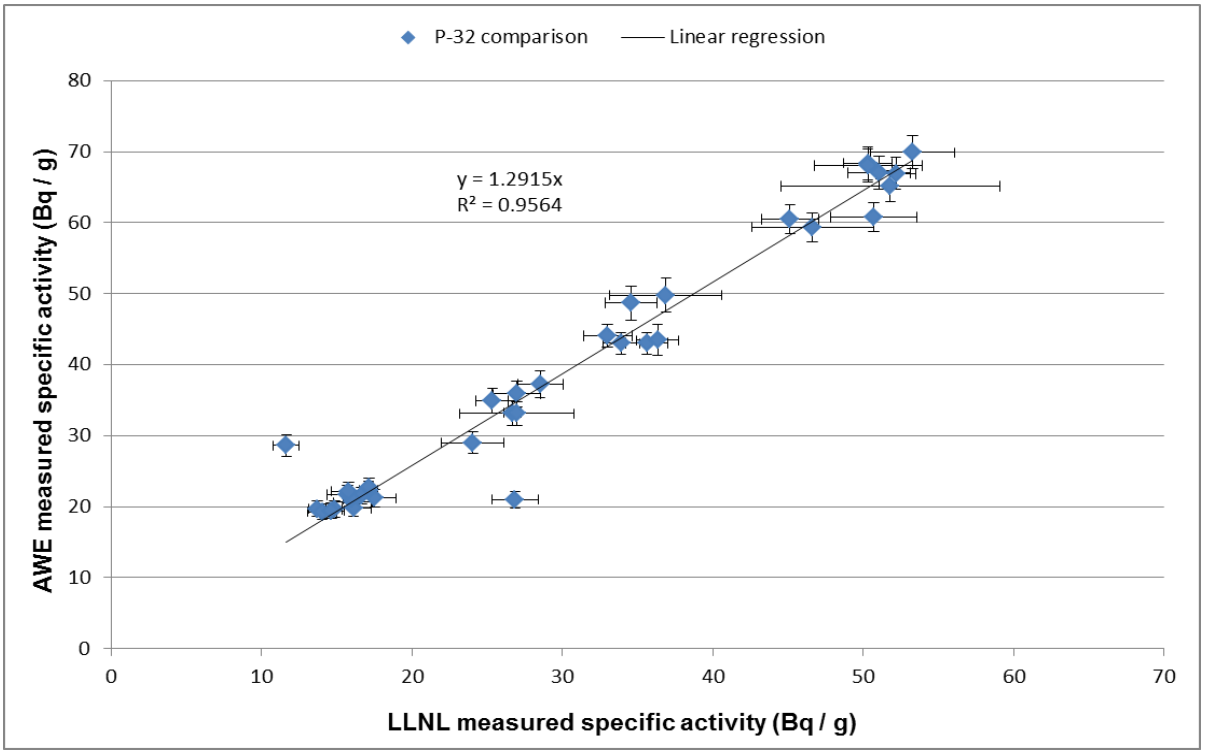

Figure C3: A scatter plot of the specific activity of P-32 measured in the sulphur component of AWE and LLNL NADs.

The specific activity may vary between the different NADs, but the behavior of the activity as a function of height is consistent for both systems. Figure shows the specific activity of ^{32}P for a range of heights, relative to its maximum value for each reference location, for both the AWE and LLNL NADs. The behavior is identical within the uncertainty of the measurement and this similarity is replicated at the other measurement locations. The data provides confidence that the observed effect in the decrease of the ^{32}P activity as a function of height is not an artefact of the measurement technique. In addition, the similarity between the points on plates A and B (182 cm) and C and D (136 cm) demonstrates that there is not a significant drop in the fluence of fast neutrons over this interval in height. In fact, there was a small vertical displacement between the AWE and LLNL NADs, of the order of 1 – 2 cm but this is not significant over the full range of heights considered. As the distance to the Godiva assembly increases the inverse square law has a smaller effect on the magnitude of the induced activity at different heights, such that at 4 m the specific activity of P-32 is constant within the uncertainty of the measurement.

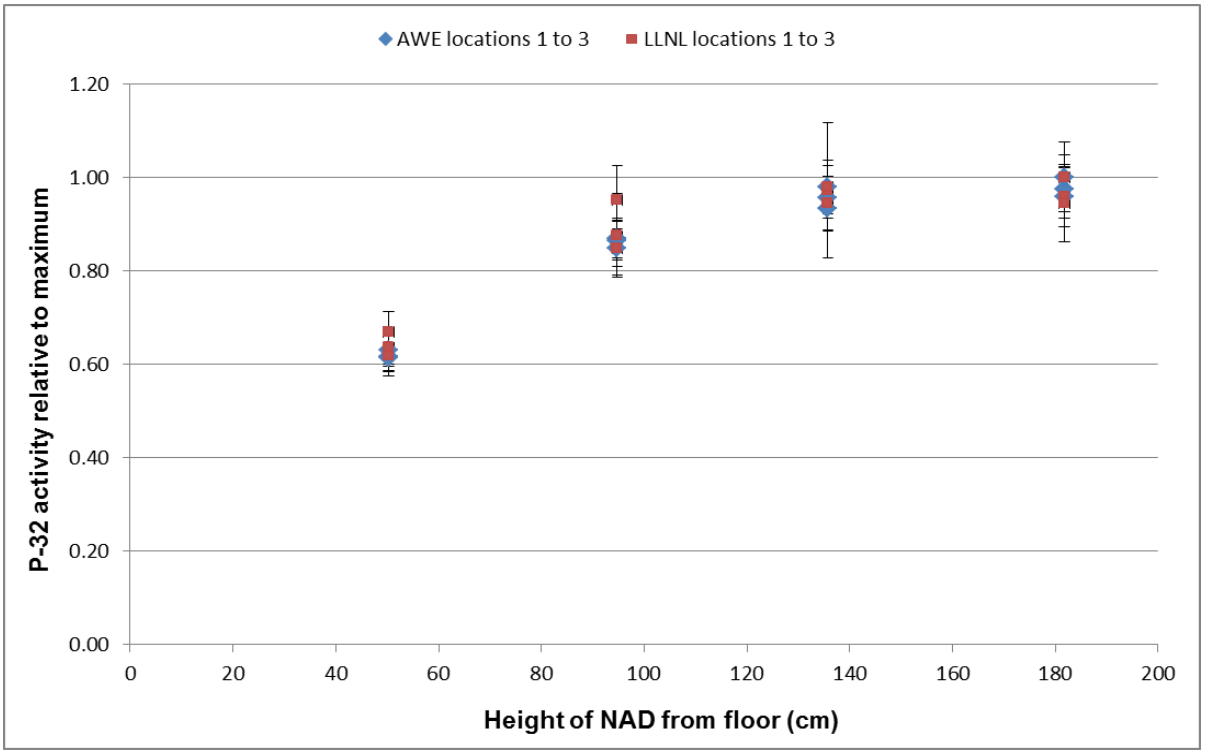

Figure C4: The behavior of the specific activity of P-32 in the sulphur component of the AWE and LLNL NADs as a function of the height of the NAD during irradiation.

Neutron-induced In-115m activity

A similar analysis was performed for the ^{115m}In activity induced in the indium component of the AWE and LLNL NADs. A scatter plot of the specific activities of ^{115m}In for the two types of NAD is shown in Figure ; the relationship is close to one-to-one, with the small deviation attributable to differences in the calibration of the gamma-ray detectors. There were some issues with the AWE measurement of the ^{115m}In activity and this is reflected in the large uncertainties and the large spread on the highest activities, which is reflected in the doses derived from the AWE NADs. Figure shows the variation in the ^{115m}In specific activity as a function of height for reference locations 1 to 3. There is disagreement between the AWE and LLNL data for these locations; the LLNL data has a similar trend to the ^{32}P data whereas the AWE data indicates an increase in the ^{115m}In activity as the height decreases. The AWE data would be consistent with a softening of the field caused by reflection of fast neutrons from the floor of the irradiation cell however the relatively large uncertainty on the data makes reduces its weight relative to the LLNL data, which does not support the same conclusion.

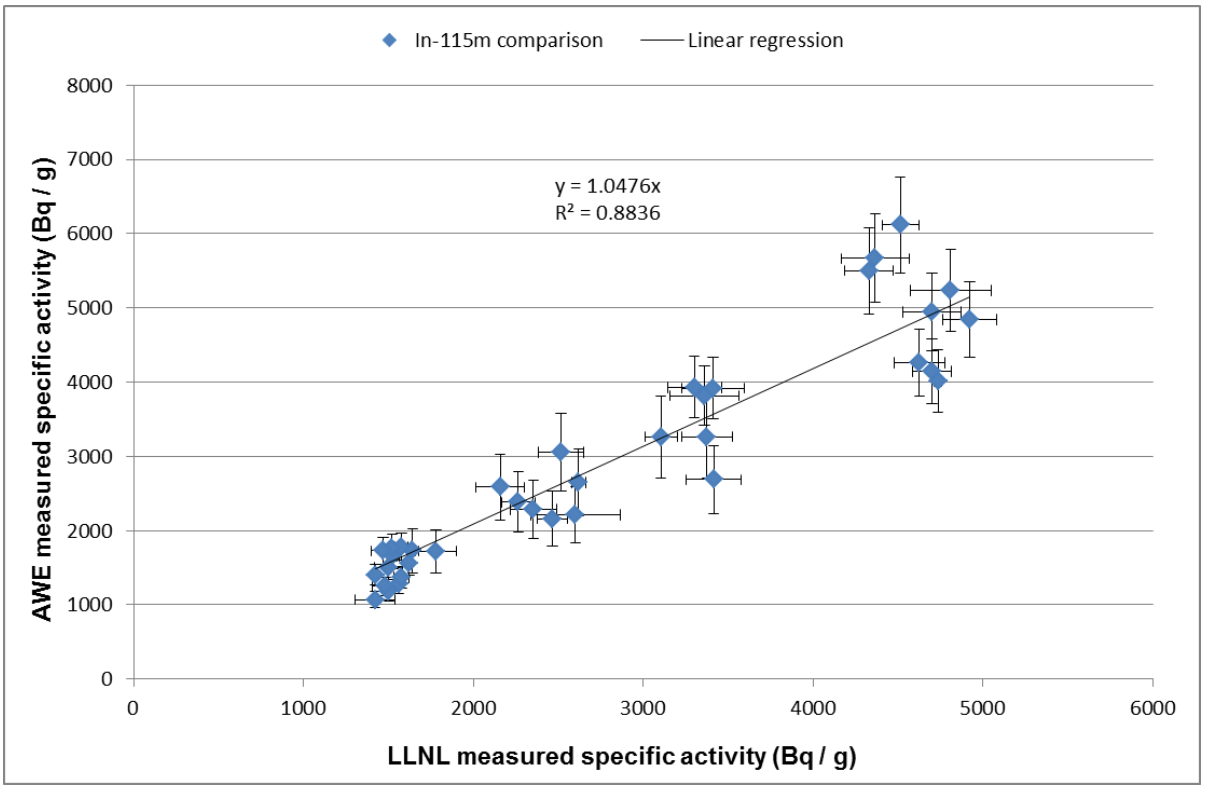

Figure C5. A scatter plot of the specific activity of In-115m measured in the indium component of AWE and LLNL NADs.

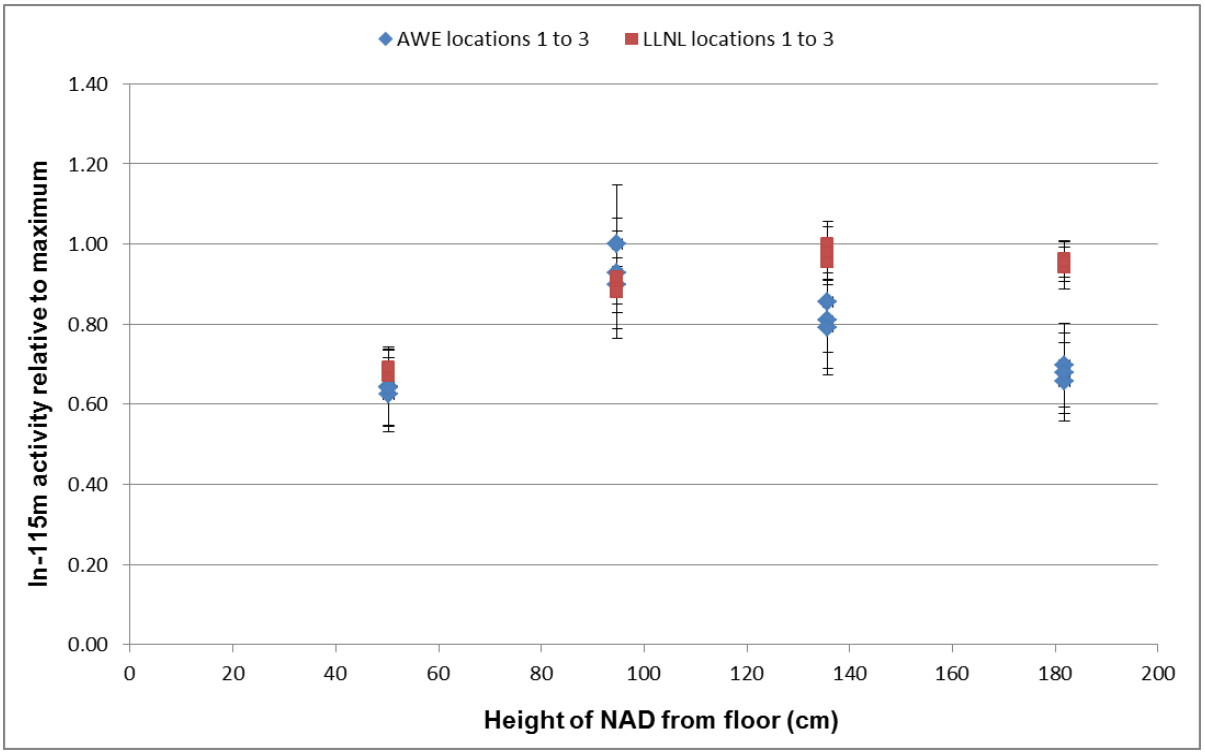

Figure C6: The behavior of the specific activity of In-115m in the indium component of the AWE and LLNL NADs as a function of the height of the NAD during irradiation.

Appendix D. PBSS deployment information and results

(From AWE Report 880-14 dated 07-November-2014)

Table D1. Information on the excursions of Godiva during the two-week campaign

Pulse No.	Date	Time	Temperature (deg. C)	Content
1	19/05/14	14:29:00	66	Bonner Spheres
2	20/05/14	10:52:10	68.8	Bonner Spheres
3	20/05/14	14:38:15	65.1	Bonner Spheres
4	21/05/14	09:42:20	65.4	Bonner Spheres
5	21/05/14	13:00:15	70	Bonner Spheres
6	21/05/14	16:09:47	70.8	Bonner Spheres
7	22/05/14	09:55:08	69.9	Bonner Spheres
8	22/05/14	13:00:21	70.6	Bonner Spheres
9	22/05/14	16:07:37	70.3	Bonner Spheres
10	27/05/14	13:31:40	230	NADs+CAD lockets + Bare Foils
11	28/05/14	10:53:00	137	NADs
12	28/05/14	15:46:05	69.2	Bonner Spheres
13	29/05/14	10:15:00	71.1	NADs
14	29/05/14	13:45:10	68.5	Bonner Spheres

Table D2. The locations of each sphere for each pulse of the Godiva reactor

Position	Pulse number											
	1	2	3	4	5	6	7	8	9	10	12	14
1	2.5"	3"	4"	5"	6"	7"	8"	10"	12"	0"	3"	3"
2	3"	4"	5"	6"	7"	8"	10"	12"	2.5"	0"	4"	4"
3	4"	5"	6"	7"	8"	10"	12"	2.5"	3"	0"	5"	5"
4	5"	6"	7"	8"	10"	12"	2.5"	3"	4"	0"	6"	6"
5	6"	7"	8"	10"	12"	2.5"	3"	4"	5"	0"	7"	7"
6	7"	8"	10"	12"	2.5"	3"	4"	5"	6"	0"	8"	8"
7	8"	10"	12"	2.5"	3"	4"	5"	6"	7"	0"	10"	10"
8	10"	12"	2.5"	3"	4"	5"	6"	7"	8"	0"	12"	12"
9	12"	2.5"	3"	4"	5"	6"	7"	8"	10"	0"	2.5"	2.5"

Table D3. Fluence data for position 1

Energy MeV	Lethargy E * Ψ(E)	Energy MeV	Lethargy E * Ψ(E)	Energy MeV	Lethargy E * Ψ(E)	Energy MeV	Lethargy E * Ψ(E)
1.58E-09	6.832E+05	5.72E-02	2.592E+09	4.66E-01	1.706E+10	3.48E+00	9.521E+09
2.51E-09	4.971E+06	6.51E-02	3.512E+09	5.18E-01	2.271E+10	3.96E+00	6.229E+09
3.98E-09	3.568E+07	7.39E-02	3.354E+09	6.01E-01	2.146E+10	4.73E+00	8.479E+09
6.31E-09	1.742E+08	8.37E-02	4.076E+09	6.71E-01	2.716E+10	5.31E+00	4.725E+09
1.00E-08	6.614E+08	9.55E-02	3.160E+09	7.41E-01	2.676E+10	5.88E+00	1.827E+09
1.58E-08	1.529E+09	1.08E-01	4.518E+09	8.25E-01	3.047E+10	6.43E+00	2.257E+09
2.51E-08	2.869E+09	1.23E-01	4.201E+09	9.16E-01	2.885E+10	6.98E+00	2.746E+09
3.98E-08	4.129E+09	1.40E-01	5.430E+09	1.02E+00	2.468E+10	7.52E+00	2.457E+09
6.31E-08	4.535E+09	1.58E-01	5.075E+09	1.13E+00	3.568E+10	8.04E+00	1.891E+09
1.00E-07	4.648E+09	2.01E-01	7.032E+09	1.26E+00	3.125E+10	8.56E+00	0.000E+00
1.58E-07	3.870E+09	2.22E-01	7.781E+09	1.42E+00	2.819E+10	9.07E+00	0.000E+00
2.51E-07	2.488E+09	2.47E-01	1.046E+10	1.61E+00	2.207E+10	9.57E+00	0.000E+00
3.98E-07	1.651E+09	2.74E-01	9.161E+09	1.85E+00	2.748E+10	1.06E+01	0.000E+00
6.31E-07	1.562E+09	3.05E-01	1.271E+10	2.09E+00	2.855E+10	1.16E+01	0.000E+00
1.00E-06	1.621E+09	3.38E-01	1.202E+10	2.38E+00	1.319E+10	1.45E+01	0.000E+00
1.00E-02	2.286E+09	3.78E-01	1.597E+10	2.69E+00	1.549E+10		
5.04E-02	3.173E+09	4.21E-01	1.855E+10	3.07E+00	1.950E+10		

Table D4. Fluence data for position 2

Energy MeV	Lethargy E * Ψ(E)	Energy MeV	Lethargy E * Ψ(E)	Energy MeV	Lethargy E * Ψ(E)	Energy MeV	Lethargy E * Ψ(E)
1.58E-09	6.153E+05	5.72E-02	2.476E+09	4.66E-01	1.631E+10	3.48E+00	9.163E+09
2.51E-09	4.354E+06	6.51E-02	3.355E+09	5.18E-01	2.172E+10	3.96E+00	5.994E+09
3.98E-09	3.143E+07	7.39E-02	3.204E+09	6.01E-01	2.055E+10	4.73E+00	8.158E+09
6.31E-09	1.544E+08	8.37E-02	3.893E+09	6.71E-01	2.602E+10	5.31E+00	4.545E+09
1.00E-08	5.908E+08	9.55E-02	3.017E+09	7.41E-01	2.563E+10	5.88E+00	1.756E+09
1.58E-08	1.375E+09	1.08E-01	4.314E+09	8.25E-01	2.921E+10	6.43E+00	2.169E+09
2.51E-08	2.600E+09	1.23E-01	4.012E+09	9.16E-01	2.770E+10	6.98E+00	2.639E+09
3.98E-08	3.771E+09	1.40E-01	5.184E+09	1.02E+00	2.369E+10	7.52E+00	2.361E+09
6.31E-08	4.174E+09	1.58E-01	4.845E+09	1.13E+00	3.426E+10	8.04E+00	1.817E+09
1.00E-07	4.309E+09	2.01E-01	6.713E+09	1.26E+00	3.000E+10	8.56E+00	0.000E+00
1.58E-07	3.609E+09	2.22E-01	7.429E+09	1.42E+00	2.710E+10	9.07E+00	0.000E+00
2.51E-07	2.335E+09	2.47E-01	9.988E+09	1.61E+00	2.123E+10	9.57E+00	0.000E+00
3.98E-07	1.556E+09	2.74E-01	8.747E+09	1.85E+00	2.643E+10	1.06E+01	0.000E+00
6.31E-07	1.475E+09	3.05E-01	1.213E+10	2.09E+00	2.747E+10	1.16E+01	0.000E+00
1.00E-06	1.529E+09	3.38E-01	1.148E+10	2.38E+00	1.269E+10	1.45E+01	0.000E+00
1.00E-02	2.179E+09	3.78E-01	1.526E+10	2.69E+00	1.491E+10		
5.04E-02	3.034E+09	4.21E-01	1.773E+10	3.07E+00	1.877E+10		

Table D5. Fluence data for position 3

Energy MeV	Lethargy E * Ψ(E)	Energy MeV	Lethargy E * Ψ(E)	Energy MeV	Lethargy E * Ψ(E)	Energy MeV	Lethargy E * Ψ(E)
1.58E-09	5.983E+05	5.72E-02	2.666E+09	4.66E-01	1.717E+10	3.48E+00	9.358E+09
2.51E-09	4.065E+06	6.51E-02	3.612E+09	5.18E-01	2.282E+10	3.96E+00	6.107E+09
3.98E-09	2.959E+07	7.39E-02	3.450E+09	6.01E-01	2.152E+10	4.73E+00	8.313E+09
6.31E-09	1.470E+08	8.37E-02	4.183E+09	6.71E-01	2.724E+10	5.31E+00	4.627E+09
1.00E-08	5.686E+08	9.55E-02	3.234E+09	7.41E-01	2.684E+10	5.88E+00	1.782E+09
1.58E-08	1.339E+09	1.08E-01	4.624E+09	8.25E-01	3.052E+10	6.43E+00	2.201E+09
2.51E-08	2.563E+09	1.23E-01	4.300E+09	9.16E-01	2.884E+10	6.98E+00	2.677E+09
3.98E-08	3.769E+09	1.40E-01	5.536E+09	1.02E+00	2.467E+10	7.52E+00	2.396E+09
6.31E-08	4.233E+09	1.58E-01	5.164E+09	1.13E+00	3.568E+10	8.04E+00	1.844E+09
1.00E-07	4.435E+09	2.01E-01	7.155E+09	1.26E+00	3.124E+10	8.56E+00	0.000E+00
1.58E-07	3.766E+09	2.22E-01	7.868E+09	1.42E+00	2.806E+10	9.07E+00	0.000E+00
2.51E-07	2.471E+09	2.47E-01	1.058E+10	1.61E+00	2.193E+10	9.57E+00	0.000E+00
3.98E-07	1.668E+09	2.74E-01	9.264E+09	1.85E+00	2.731E+10	1.06E+01	0.000E+00
6.31E-07	1.595E+09	3.05E-01	1.285E+10	2.09E+00	2.833E+10	1.16E+01	0.000E+00
1.00E-06	1.660E+09	3.38E-01	1.211E+10	2.38E+00	1.301E+10	1.45E+01	0.000E+00
1.00E-02	2.398E+09	3.78E-01	1.607E+10	2.69E+00	1.528E+10		
5.04E-02	3.295E+09	4.21E-01	1.867E+10	3.07E+00	1.923E+10		

Table D6. Fluence data for position 4

Energy MeV	Lethargy E * Ψ(E)	Energy MeV	Lethargy E * Ψ(E)	Energy MeV	Lethargy E * Ψ(E)	Energy MeV	Lethargy E * Ψ(E)
1.58E-09	4.689E+05	5.72E-02	1.896E+09	4.66E-01	1.108E+10	3.48E+00	4.810E+09
2.51E-09	3.484E+06	6.51E-02	2.568E+09	5.18E-01	1.443E+10	3.96E+00	3.130E+09
3.98E-09	2.503E+07	7.39E-02	2.453E+09	6.01E-01	1.318E+10	4.73E+00	4.260E+09
6.31E-09	1.222E+08	8.37E-02	2.959E+09	6.71E-01	1.669E+10	5.31E+00	2.375E+09
1.00E-08	4.646E+08	9.55E-02	2.272E+09	7.41E-01	1.644E+10	5.88E+00	9.197E+08
1.58E-08	1.075E+09	1.08E-01	3.248E+09	8.25E-01	1.831E+10	6.43E+00	1.136E+09
2.51E-08	2.025E+09	1.23E-01	3.020E+09	9.16E-01	1.658E+10	6.98E+00	1.382E+09
3.98E-08	2.937E+09	1.40E-01	3.841E+09	1.02E+00	1.418E+10	7.52E+00	1.237E+09
6.31E-08	3.263E+09	1.58E-01	3.560E+09	1.13E+00	2.051E+10	8.04E+00	9.517E+08
1.00E-07	3.392E+09	2.01E-01	4.932E+09	1.26E+00	1.796E+10	8.56E+00	0.000E+00
1.58E-07	2.865E+09	2.22E-01	5.284E+09	1.42E+00	1.539E+10	9.07E+00	0.000E+00
2.51E-07	1.876E+09	2.47E-01	7.104E+09	1.61E+00	1.182E+10	9.57E+00	0.000E+00
3.98E-07	1.275E+09	2.74E-01	6.222E+09	1.85E+00	1.472E+10	1.06E+01	0.000E+00
6.31E-07	1.234E+09	3.05E-01	8.629E+09	2.09E+00	1.516E+10	1.16E+01	0.000E+00
1.00E-06	1.305E+09	3.38E-01	7.885E+09	2.38E+00	6.717E+09	1.45E+01	0.000E+00
1.00E-02	1.876E+09	3.78E-01	1.037E+10	2.69E+00	7.891E+09		
5.04E-02	2.386E+09	4.21E-01	1.205E+10	3.07E+00	9.932E+09		

Table D7. Fluence data for position 5

Energy MeV	Lethargy E * Ψ(E)	Energy MeV	Lethargy E * Ψ(E)	Energy MeV	Lethargy E * Ψ(E)	Energy MeV	Lethargy E * Ψ(E)
1.58E-09	4.973E+05	5.72E-02	1.995E+09	4.66E-01	1.162E+10	3.48E+00	4.772E+09
2.51E-09	3.742E+06	6.51E-02	2.703E+09	5.18E-01	1.505E+10	3.96E+00	3.107E+09
3.98E-09	2.682E+07	7.39E-02	2.581E+09	6.01E-01	1.364E+10	4.73E+00	4.229E+09
6.31E-09	1.306E+08	8.37E-02	3.115E+09	6.71E-01	1.727E+10	5.31E+00	2.361E+09
1.00E-08	4.946E+08	9.55E-02	2.394E+09	7.41E-01	1.701E+10	5.88E+00	9.184E+08
1.58E-08	1.141E+09	1.08E-01	3.423E+09	8.25E-01	1.885E+10	6.43E+00	1.134E+09
2.51E-08	2.143E+09	1.23E-01	3.183E+09	9.16E-01	1.691E+10	6.98E+00	1.380E+09
3.98E-08	3.099E+09	1.40E-01	4.055E+09	1.02E+00	1.446E+10	7.52E+00	1.235E+09
6.31E-08	3.435E+09	1.58E-01	3.761E+09	1.13E+00	2.091E+10	8.04E+00	9.504E+08
1.00E-07	3.563E+09	2.01E-01	5.212E+09	1.26E+00	1.831E+10	8.56E+00	0.000E+00
1.58E-07	3.004E+09	2.22E-01	5.571E+09	1.42E+00	1.550E+10	9.07E+00	0.000E+00
2.51E-07	1.964E+09	2.47E-01	7.490E+09	1.61E+00	1.186E+10	9.57E+00	0.000E+00
3.98E-07	1.333E+09	2.74E-01	6.560E+09	1.85E+00	1.476E+10	1.06E+01	0.000E+00
6.31E-07	1.289E+09	3.05E-01	9.098E+09	2.09E+00	1.517E+10	1.16E+01	0.000E+00
1.00E-06	1.365E+09	3.38E-01	8.281E+09	2.38E+00	6.658E+09	1.45E+01	0.000E+00
1.00E-02	1.971E+09	3.78E-01	1.088E+10	2.69E+00	7.823E+09		
5.04E-02	2.502E+09	4.21E-01	1.264E+10	3.07E+00	9.846E+09		

Table D8: Fluence data for position 6

Energy MeV	Lethargy E * Ψ(E)	Energy MeV	Lethargy E * Ψ(E)	Energy MeV	Lethargy E * Ψ(E)	Energy MeV	Lethargy E * Ψ(E)
1.58E-09	5.603E+05	5.72E-02	2.631E+09	4.66E-01	1.517E+10	3.48E+00	5.727E+09
2.51E-09	3.993E+06	6.51E-02	3.565E+09	5.18E-01	1.963E+10	3.96E+00	3.685E+09
3.98E-09	2.895E+07	7.39E-02	3.404E+09	6.01E-01	1.777E+10	4.73E+00	5.015E+09
6.31E-09	1.430E+08	8.37E-02	4.104E+09	6.71E-01	2.249E+10	5.31E+00	2.784E+09
1.00E-08	5.501E+08	9.55E-02	3.150E+09	7.41E-01	2.215E+10	5.88E+00	1.062E+09
1.58E-08	1.288E+09	1.08E-01	4.503E+09	8.25E-01	2.449E+10	6.43E+00	1.312E+09
2.51E-08	2.457E+09	1.23E-01	4.188E+09	9.16E-01	2.185E+10	6.98E+00	1.596E+09
3.98E-08	3.611E+09	1.40E-01	5.314E+09	1.02E+00	1.869E+10	7.52E+00	1.428E+09
6.31E-08	4.068E+09	1.58E-01	4.921E+09	1.13E+00	2.702E+10	8.04E+00	1.099E+09
1.00E-07	4.290E+09	2.01E-01	6.818E+09	1.26E+00	2.366E+10	8.56E+00	0.000E+00
1.58E-07	3.669E+09	2.22E-01	7.271E+09	1.42E+00	1.966E+10	9.07E+00	0.000E+00
2.51E-07	2.434E+09	2.47E-01	9.776E+09	1.61E+00	1.493E+10	9.57E+00	0.000E+00
3.98E-07	1.673E+09	2.74E-01	8.561E+09	1.85E+00	1.859E+10	1.06E+01	0.000E+00
6.31E-07	1.631E+09	3.05E-01	1.187E+10	2.09E+00	1.900E+10	1.16E+01	0.000E+00
1.00E-06	1.729E+09	3.38E-01	1.081E+10	2.38E+00	8.132E+09	1.45E+01	0.000E+00
1.00E-02	2.542E+09	3.78E-01	1.419E+10	2.69E+00	9.554E+09		
5.04E-02	3.313E+09	4.21E-01	1.649E+10	3.07E+00	1.202E+10		

Table D9. Fluence data for position 7

Energy MeV	Lethargy E * Ψ(E)	Energy MeV	Lethargy E * Ψ(E)	Energy MeV	Lethargy E * Ψ(E)	Energy MeV	Lethargy E * Ψ(E)
1.58E-09	4.116E+05	5.72E-02	1.596E+09	4.66E-01	8.196E+09	3.48E+00	3.240E+09
2.51E-09	3.061E+06	6.51E-02	2.162E+09	5.18E-01	1.064E+10	3.96E+00	2.095E+09
3.98E-09	2.198E+07	7.39E-02	2.065E+09	6.01E-01	9.685E+09	4.73E+00	2.852E+09
6.31E-09	1.073E+08	8.37E-02	2.344E+09	6.71E-01	1.226E+10	5.31E+00	1.587E+09
1.00E-08	4.077E+08	9.55E-02	1.658E+09	7.41E-01	1.208E+10	5.88E+00	6.109E+08
1.58E-08	9.429E+08	1.08E-01	2.371E+09	8.25E-01	1.338E+10	6.43E+00	7.546E+08
2.51E-08	1.775E+09	1.23E-01	2.205E+09	9.16E-01	1.198E+10	6.98E+00	9.181E+08
3.98E-08	2.572E+09	1.40E-01	2.813E+09	1.02E+00	1.025E+10	7.52E+00	8.216E+08
6.31E-08	2.856E+09	1.58E-01	2.611E+09	1.13E+00	1.482E+10	8.04E+00	6.322E+08
1.00E-07	2.966E+09	2.01E-01	3.618E+09	1.26E+00	1.297E+10	8.56E+00	0.000E+00
1.58E-07	2.503E+09	2.22E-01	3.897E+09	1.42E+00	1.088E+10	9.07E+00	0.000E+00
2.51E-07	1.637E+09	2.47E-01	5.240E+09	1.61E+00	8.291E+09	9.57E+00	0.000E+00
3.98E-07	1.111E+09	2.74E-01	4.589E+09	1.85E+00	1.032E+10	1.06E+01	0.000E+00
6.31E-07	1.074E+09	3.05E-01	6.364E+09	2.09E+00	1.057E+10	1.16E+01	0.000E+00
1.00E-06	1.134E+09	3.38E-01	5.828E+09	2.38E+00	4.567E+09	1.45E+01	0.000E+00
1.00E-02	1.633E+09	3.78E-01	7.670E+09	2.69E+00	5.365E+09		
5.04E-02	2.103E+09	4.21E-01	8.911E+09	3.07E+00	6.753E+09		

Table D10: Fluence data for position 8

Energy MeV	Lethargy E * Ψ(E)	Energy MeV	Lethargy E * Ψ(E)	Energy MeV	Lethargy E * Ψ(E)	Energy MeV	Lethargy E * Ψ(E)
1.58E-09	4.321E+05	5.72E-02	1.690E+09	4.66E-01	8.736E+09	3.48E+00	3.205E+09
2.51E-09	3.224E+06	6.51E-02	2.289E+09	5.18E-01	1.130E+10	3.96E+00	2.067E+09
3.98E-09	2.315E+07	7.39E-02	2.186E+09	6.01E-01	1.021E+10	4.73E+00	2.813E+09
6.31E-09	1.129E+08	8.37E-02	2.494E+09	6.71E-01	1.293E+10	5.31E+00	1.566E+09
1.00E-08	4.287E+08	9.55E-02	1.777E+09	7.41E-01	1.273E+10	5.88E+00	6.025E+08
1.58E-08	9.908E+08	1.08E-01	2.541E+09	8.25E-01	1.402E+10	6.43E+00	7.442E+08
2.51E-08	1.864E+09	1.23E-01	2.363E+09	9.16E-01	1.240E+10	6.98E+00	9.055E+08
3.98E-08	2.702E+09	1.40E-01	3.017E+09	1.02E+00	1.061E+10	7.52E+00	8.103E+08
6.31E-08	2.999E+09	1.58E-01	2.803E+09	1.13E+00	1.534E+10	8.04E+00	6.235E+08
1.00E-07	3.115E+09	2.01E-01	3.883E+09	1.26E+00	1.344E+10	8.56E+00	0.000E+00
1.58E-07	2.629E+09	2.22E-01	4.175E+09	1.42E+00	1.109E+10	9.07E+00	0.000E+00
2.51E-07	1.720E+09	2.47E-01	5.614E+09	1.61E+00	8.403E+09	9.57E+00	0.000E+00
3.98E-07	1.169E+09	2.74E-01	4.916E+09	1.85E+00	1.046E+10	1.06E+01	0.000E+00
6.31E-07	1.131E+09	3.05E-01	6.818E+09	2.09E+00	1.068E+10	1.16E+01	0.000E+00
1.00E-06	1.197E+09	3.38E-01	6.220E+09	2.38E+00	4.535E+09	1.45E+01	0.000E+00
1.00E-02	1.741E+09	3.78E-01	8.175E+09	2.69E+00	5.328E+09		
5.04E-02	2.250E+09	4.21E-01	9.497E+09	3.07E+00	6.706E+09		

Table D11. Fluence data for position 9

Energy MeV	Lethargy E * Ψ(E)	Energy MeV	Lethargy E * Ψ(E)	Energy MeV	Lethargy E * Ψ(E)	Energy MeV	Lethargy E * Ψ(E)
1.58E-09	4.494E+05	5.72E-02	1.756E+09	4.66E-01	8.837E+09	3.48E+00	3.143E+09
2.51E-09	3.392E+06	6.51E-02	2.380E+09	5.18E-01	1.140E+10	3.96E+00	2.021E+09
3.98E-09	2.431E+07	7.39E-02	2.273E+09	6.01E-01	1.027E+10	4.73E+00	2.752E+09
6.31E-09	1.184E+08	8.37E-02	2.579E+09	6.71E-01	1.301E+10	5.31E+00	1.529E+09
1.00E-08	4.485E+08	9.55E-02	1.823E+09	7.41E-01	1.281E+10	5.88E+00	5.861E+08
1.58E-08	1.034E+09	1.08E-01	2.607E+09	8.25E-01	1.409E+10	6.43E+00	7.240E+08
2.51E-08	1.944E+09	1.23E-01	2.424E+09	9.16E-01	1.242E+10	6.98E+00	8.808E+08
3.98E-08	2.814E+09	1.40E-01	3.086E+09	1.02E+00	1.063E+10	7.52E+00	7.882E+08
6.31E-08	3.123E+09	1.58E-01	2.862E+09	1.13E+00	1.536E+10	8.04E+00	6.065E+08
1.00E-07	3.245E+09	2.01E-01	3.966E+09	1.26E+00	1.345E+10	8.56E+00	0.000E+00
1.58E-07	2.742E+09	2.22E-01	4.244E+09	1.42E+00	1.104E+10	9.07E+00	0.000E+00
2.51E-07	1.797E+09	2.47E-01	5.705E+09	1.61E+00	8.343E+09	9.57E+00	0.000E+00
3.98E-07	1.225E+09	2.74E-01	4.996E+09	1.85E+00	1.039E+10	1.06E+01	0.000E+00
6.31E-07	1.190E+09	3.05E-01	6.929E+09	2.09E+00	1.059E+10	1.16E+01	0.000E+00
1.00E-06	1.264E+09	3.38E-01	6.299E+09	2.38E+00	4.466E+09	1.45E+01	0.000E+00
1.00E-02	1.833E+09	3.78E-01	8.270E+09	2.69E+00	5.247E+09		
5.04E-02	2.327E+09	4.21E-01	9.607E+09	3.07E+00	6.604E+09		